

Copyright is owned by the Author of the thesis. Permission is given for a copy to be downloaded by an individual for the purpose of research and private study only. The thesis may not be reproduced elsewhere without the permission of the Author.

**Design of attitude determination and control system for
KIWISAT amateur satellite.**

A thesis presented in partial fulfillment of
the requirements for degree of

**Masters of Engineering
Mechatronics**

At

Massey University
Albany, Auckland
New Zealand

Abstract

This thesis is to present the design of “ADAC” system for “KiwiSat” cube satellite. An array of sensors were used: CMOS low resolution camera, sun sensor, earth horizon sensors, 3 axis magnetometer. The control of satellite rely on magnetic coils installed orthogonally to each other. Implementation of this system is essential to achieve the full control of the satellite when it reaches the lower orbit.

Solution for the pitfall such as: the lack of torque of the satellite when it’s parallel to the earth magnetic field, was also designed. Attitude estimation is nonlinear due of kinematics and the reading of above sensors.

Both a proportional-derivative controller and a linear quadratic regulator are implemented for control model of the system. And the Floquet Theory is used to check the stability of the controls, and an optimization method further optimizes the results.

Model was constructed by simulink program that was packaged with mathematical software called “Matlab”.

3D model of the satellite was drawn in SolidWorks for the purpose of visual interaction and behavior.

Acknowledgments

I would like to thank everyone who provided me with support and help in the time of this project.

Firstly I would like to thank my family: my dad Alex Makarov, my mum Elena Makarova and my little brother Dennis Makarov. They gave me great amount of support and faith in myself.

My sincere gratitude to my mentor Dr. Johan Potgieter at Institute of Technology & Engineering, Massey University, his understanding and guidance helped me through some rough stages of my Masters project. His great knowledge have been a huge amount of help to me.

My gratitude and thanks to my supervisors: Fred Kennedy and Jonathan Henderson. For their detailed structural comments and amount of help they provided.

Also I would like to thank all staff members who helped me to achieve completion on my practical part of the project.

And a big thanks to my university friends, who provided a big moral support.

Without all of you, it wouldn't be possible! Thank you guys!

Table of Contents

Chapter:

1. Introduction	1
1.1. Objectives	1
1.2. Literature overview	1
1.2.1. Magnetic field	1
1.2.2. Earth magnetic field	4
1.2.3. Spacecraft magnetic field	13
1.2.4. Literature review discussion	22
2. ADAC system for magnetically controlled satellites	23
2.1. Dynamics and Attitude determination	23
2.1.1. Spacecraft and orbit dynamics	23
2.1.2. Attitude dynamics	32
2.1.3. Attitude determination	39
2.2. Control of satellite	40
2.2.1. Control and stabilization	40
2.2.2. Control laws	41
3. Model and results	45
3.1. Mathematical model of the system	45
3.2. Animation	53
3.3. Results	56
4. Discussion and conclusion	62
4.1. Discussion	62
4.2. Conclusion	62
References	63

Appendix

LIST OF TABLES, FIGURES AND GRAPHS

Figure 1.1: Magnetic field of the bar magnet	3
Figure 1.2: Magnetic field Units	4
Figure 1.3: Magnetic field Strengths	5
Figure 1.4: Magnetic field model	6
Figure 1.5: Geomagnetic Coordinates	6
Figure 1.6: The Magnetosphere	7
Figure 1.7: Appearance and Evolution of a Magnetic wave	11
Figure 1.8: Movement of the North Pole over Time	12
Figure 1.9: Movement of the South Pole over Time	12
Figure 1.10: Forces on the Moving Charges in a Current-Carrying Conductor	13
Figure 1.11: Forces on a Current-Carrying Loop in a Magnetic	15
Figure 1.12: Magnetic Torque Direction	18
Figure 1.13: Magnetic control torque	19
Figure 1.14: Equatorial Orbit in Magnetic field	21
Figure 1.15: polar orbit in Magnetic Field	22
Figure 2.1: Relative Motion of Two Bodies	25
Figure 2.2: Values of eccentricity and Elliptical orbit	27- 28
Figure 2.3: Orbital Elements	28
Figure 2.4: Heliocentric-Ecliptic Coordinate System	30
Figure 2.5: Earth-Centered Inertial reference Frame	31
Figure 2.6: Earth-Centered Earth-Fixed Reference Frame	32
Figure 2.7: Earth-Centered Inertial and Orbital Reference Frame	33

Figure 2.8: Ranges of sensor Accuracy	39
Figure 2.9: Summary of LQR Method	44
Figure 3.1: Designed dynamics system of amateur satellite	45
Figure 3.2: The simulation model	46
Figure 3.3: Attitude determination and control box	46
Figure 3.4: Embedded Block Diagram	47
Figure 3.5: Angular velocity stabilization.....	48
Figure 3.6: Behavior of satellite	49
Figure 3.7: Attitude matrix	50
Figure 3.8: 3D model of the satellite	53
Figure 3.9: Quaternions with No Magnetic Torque, Initial Angle=14	57
Figure 3.10: Quaternions with No Magnetic Torque, Initial Angle=6	58
Figure 3.11: Quaternion for P-D Controller with assigned gains	59
Figure 3.12: Eigenvalues of $X(t)$	60
Figure 3.13: Quaternion for Linear, LQR Controller	60
Figure 3.14: Magnetic Moment	61

LIST OF SYMBOLS

H - Magnetic field of a bar magnet

r - Distance between the magnetic field source and the measurement point

\hat{a}_r - Unit vector from the center of the magnet to the measurement point

M - Magnetic dipole moment of the bar magnet

\mathcal{M} - Magnetization

B - Flux density

μ_0 - Magnetization and the permeability of free space

R_{\oplus} - Radius of the Earth

F - Force

q_1, q_2 - Electrical charges

v_1, v_2 - Drift velocity of the positive charge

n_i - Number of positive charges

A_w - Cross-sectional area of the wire

l_w - Length of the wire

J - Current density

I - Current

B_k - Component of the field which is parallel to the wire

N - Number of turns of wire

μ - Permeability of the core material

\hat{n} - Unit vector normal to plane of the coil

Δg_m - Undesired magnetic torque

\hat{B} - Unit vector in the direction of the magnetic field

\mathbf{m} - Mass of the object

$\Sigma \mathbf{F}$ - vector sum of the forces acting on mass of the object

$\ddot{\mathbf{r}}$ - Vector acceleration of \mathbf{m}

\mathbf{G} - Universal gravitational constant with a value of $6.670 \times 10^{-11} \text{m}^3/(\text{kg}\cdot\text{s}^2)$

μ - Gravitational parameter

\mathbf{h} - Angular momentum

ϕ_f - Flight path angle

\mathbf{p} - Semilatus parameter

\mathbf{e} - Eccentricity

a - Semi-major axis

I - Inclination (chapter 2)

Ω - Right ascension of the ascending node

ω - Argument of periapsis

T - Time of periapsis passage

Π - Longitude of periapsis

ν_0 - True anomaly at epoch

t_0 - Particular epoch

u_0 - Latitude at epoch

l_0 - The true longitude at epochs

Chapter 1

Introduction

Past few years a reasonable amount of work was spent to build Microsat class amateur communication satellite for launch into Low Earth Orbit. The name of the Satellite is "KiwiSAT". KiwiSAT's size is 240mm x 240mm x 280mm and with weight of 12 kg at launch. It's powered by solar battery system providing some 15 Watts of power. Various sensors used for determining the satellite dynamics and magnetic coils and magnetometer for control. After launch the satellite would determine and monitor the orbit position using those sensors and control using the Earth's geomagnetic field, which is discussed in literature overview section.

1.1 Objectives

The objective of this project is to analyze and design attitude determination and control method for KiwiSat satellite. To decide on most efficient control method and to determine and overcome the pitfalls such as lack of perpendicularity of magnetic moment of the satellite to the local magnetic field and/or prediction of the dynamic nature of earth magnetic field.

1.2 Literature overview

In this chapter the importance of magnetic field structure is discussed. Determination of position and control for amature satelite is discussed very detailed in this chapter too.

1.2.1 Magnetic field

Control of spacecraft that use magnetic coils is totally dependent on the earth's magnetic field. A discussion of the geomagnetic field is presented in this chapter of thesis. General information on magnetic is presented, then the discussion of earth's magnetic field, its origin, characteristics and variations. Mathematical models of the geomagnetic field using IGRF* developed and compared.

Origin and equations:

Magnetic and electric field are closely related, this relationship was determined in 1819 by Hans Christian Oersted when he discovered that the position of the needle of the compass is affected by nearby wire that have a current running through it. Twelve years later, Michael Faraday and Joseph Henry stated that electric voltage could be produced at the loops of wire by moving magnets close to it. [Obtained from reference 1](#)

Magnetic field from the motion of electrons, the orbital rotation of electrons around the nucleus of the atom and the spin of the electron about its own axis, combined give rise to magnetic field.

The basics of modern electromagnetic theory formed in Maxwell's differential and integral form equations:

$$(1.1) \quad \nabla \cdot \mathbf{E} = \frac{\rho}{\epsilon_0}$$

$$(1.2) \quad \int \mathbf{E} \cdot d\mathbf{A} = \frac{q}{\epsilon_0}$$

Equations (1.1) and (1.2), both forms of Gauss' Law for Electricity (SDSA. Its states that electric flux of isolated or closed surface is proportional to the total charge enclosed in the surface.

$$(1.3) \quad \nabla \cdot \mathbf{B} = 0$$

$$(1.4) \quad \int \mathbf{B} \cdot d\mathbf{A} = 0$$

Equations (1.3) and (1.4), forms Gauss' Law of Magnetism. Its states that magnetic flux out of any isolated or closed surface is zero. Then the magnetic flux directed inwards the South Pole is equal to the flux outward from the North Pole in a magnetic dipole of a closed or isolated surface.

$$(1.5) \quad \nabla \times \mathbf{E} = -\frac{d}{dt} \mathbf{B}$$

$$(1.6) \quad \int \mathbf{E} \cdot ds = -\frac{d\Phi_{\mathbf{B}}}{dt}$$

Equations (1.5) and (1.6), known as Faraday's Law of Induction. This law states that the integral of an electric field around a closed loop is equal to the negative rate of change of the magnetic flux through the area enclosed by the loop.

$$(1.7) \quad \nabla \times \mathbf{B} = \mu_0 \epsilon_0 \frac{d}{dt} \mathbf{E} + \mu_0 \mathbf{J}$$

$$(1.8) \quad \int \mathbf{B} \cdot d\mathbf{s} = \mu_0 I + \mu_0 \epsilon_0 \frac{d\Phi_E}{dt}$$

Equations (1.1) – (1.8) obtained from reference 1.

Equations (1.7) and (1.8), known as Ampere's Law. It states that the integral of a magnetic field around a closed loop is proportional to the electric current flowing through the loop.

Characteristics:

The magnetic field is a vector quantity, which means that it has both a magnitude and a direction. Macintyre discusses the fundamentals of magnetic fields and the relationship between magnetic quantities. A common example of a magnet and a magnetic field is that of a bar magnet, shown in **Figure 1.1**.

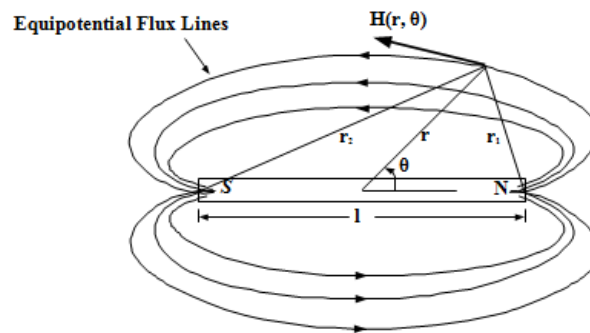


Figure 1.1: Magnetic field of the bar magnet (obtained from reference 2).

The magnetic field of a bar magnet, 'H', measured at a far distance is:

$$(1.9) \quad \mathbf{H} = \frac{3(M \times \hat{a}_r) \hat{a}_r - M}{r^3}$$

Where 'r' is the distance between the magnetic field source and the measurement point ' \hat{a}_r ', is a unit vector from the center of the magnet to the measurement point, and 'M' is the magnetic dipole moment of the bar magnet.

$$(1.10) \quad \mathcal{M} = \frac{M}{\text{volume}}$$

The magnetization, of an object is its magnetic strength or intensity, and depends on the density of its volume-distributed moments. It's a material property, and arises from both internal sources and external sources.

The relationship between the magnetic field and magnetic induction or flux density, ' \mathbf{B} ', is dependent on magnetization and the permeability of free space, ' μ_0 '

$$(1.11) \mathbf{B} = \mu_0(\mathbf{H} + \mathcal{M})$$

1.2.2 Earth magnetic field

In free space, the magnetic induction is proportional to the magnetic field by the constant factor, ' μ_0 '.

$$(1.12) \mathbf{B} = \mu_0 \mathbf{H}$$

The value of ' μ_0 ' is equal to 1 in the International System of Units (SI), so the value of the magnetic field and that of the magnetic induction are equal in free space. For the remainder of this document, ' \mathbf{B} ' is used to represent both ' \mathbf{H} ' and ' \mathbf{B} '.

Deferent units are used to represent magnetic fields. The relationship between these units is listed in **Figure 1.2**. In this Thesis unit Tesla is used.

$\mathbf{B} =$	10^4 Gauss (G)
$\mathbf{B} =$	1 Weber/meter ² (Wb/m ²)
$\mathbf{B} =$	10^3 gamma (γ)
$\mathbf{B} =$	1 Tesla (T)

Figure 1.2: Magnetic field Units.

A comparison of various magnetic field strengths is shown in **Figure 1.3**. The strongest magnetic field made by man and sustained in a lab, is approximately 40 T. The strongest naturally occurring field is found on a Magnetar, which is a type of neutron star.

Magnetic Field	Strength (Gauss)
Galactic Magnetic Field	0.00001
Solar Wind	0.00005
Interstellar Molecular Cloud	0.001
Earth's Field at Ground Level	1
Solar Surface Field	1-5
Massive Star (pre Supernova)	100
Toy Refrigerator Magnet	100
Sun Spot Field	1000
Jupiter Magnetic Field	1000
Magnetic Stars	11,500
White Dwarf Star Surfaces	1,000,000
Neutron Star Surfaces	1,000,000,000,000
Magnetar Field	1,000,000,000,000,000

Figure 1.3 : Magnetic field Strengths

Geomagnetic field:

The magnetic field around the Earth resembles that of a uniformly magnetized sphere, or a dipole, which is tilted as shown in **Figure 1.4**. The fact that it approximates a tilted dipole was discovered in 1600 by William Gilbert. In 1635, Gellibrand showed that the geomagnetic field is time and position dependent. [Information obtained from reference 3.](#)

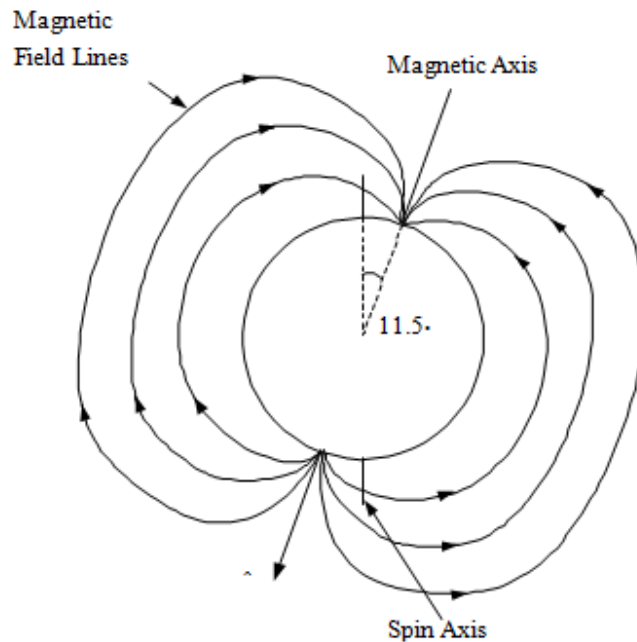


Figure 1.4: Magnetic field model

The magnetic field is weakest at the magnetic equator. The geomagnetic coordinates compared

with spin axis coordinates are shown in **Figure 1.5**.

US/UK World Magnetic Chart -- Epoch 2000 Geomagnetic Coordinates

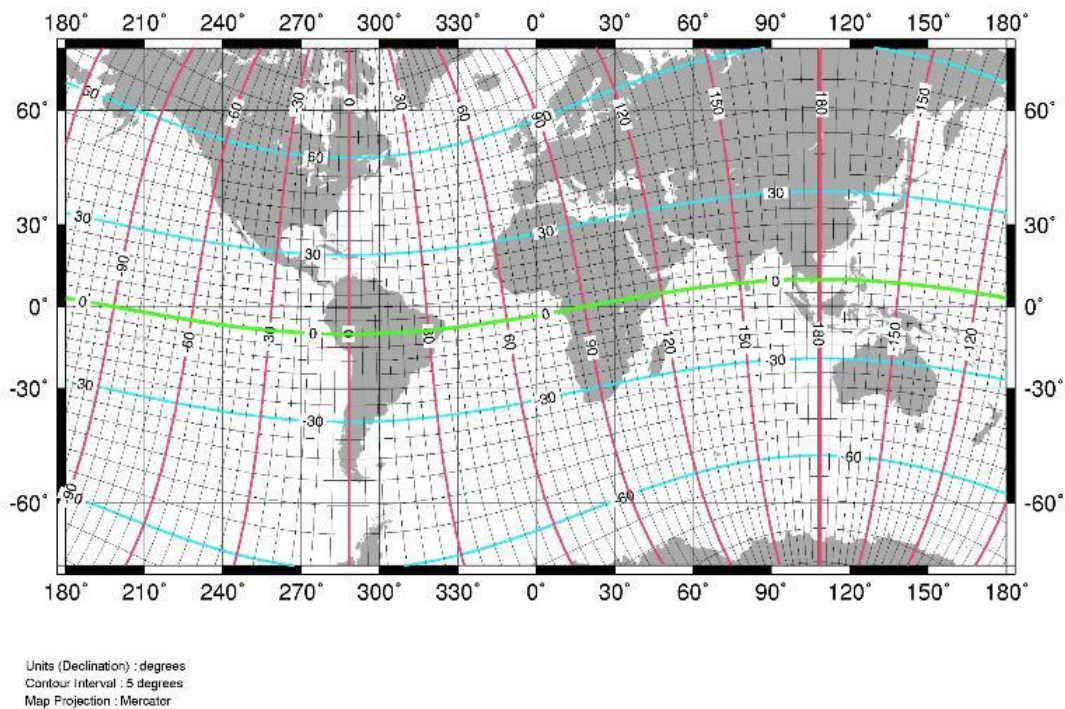


Figure 1.5: Geomagnetic Coordinates (obtained from reference 4)

At locations on the Earth's surface, a magnetic dipole model is not closely followed. However, as the altitude increases, the contours of the field strength begin to become regular and resemble a dipole field. There is a low in magnetic intensity at about 30° S, 50° W, called the Brazilian Anomaly, and a high at 10° N, 100° E. Together, these anomalies imply that the center of the dipole is offset from the center of the Earth.

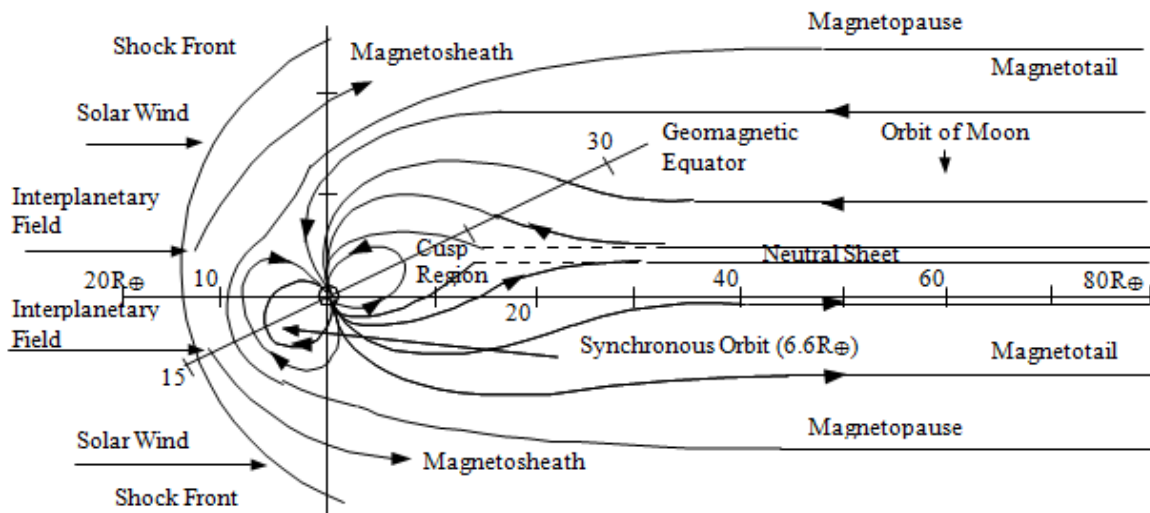


Figure 1.6: The Magnetosphere (obtained from reference 3)

The magnetosphere is created from the interaction of the solar wind, and the geomagnetic field. The two areas have a great effect on each other, with the solar wind acting to compress the Earth's magnetic field, while particles of the solar wind are deflected and trapped by the geomagnetic field. This effect causes the structure of the geomagnetic field to be complex and consist of a number of regions. More details about them:

Shock Front:

A shock front exists at the boundary between the solar wind and the geomagnetic field.

This shock is similar to a sonic boom and occurs because the solar wind is moving faster than the magnetic field can respond. The magnetic field experiences oscillations with large amplitudes at this location. These oscillations can be as large as 10 to 50 nT, whereas on either side of the shock front they usually fall in the range of 2 to 5 nT. Additionally, the oscillations occur at a higher frequency at the shock front. Information obtained from reference 3.

Magnetosheath:

The magnetosheath is a region of turbulence where the solar wind is deflected after passing through the shock front. The field inside the magnetosheath fluctuates rapidly, both in strength and direction. In the direction towards the sun, the magnetosheath is nominally $4 R_{\oplus}$, where R_{\oplus} is the radius of the Earth. However, it can shrink to approximately $2 R_{\oplus}$ during a magnetic storm occurring during a year of low solar activity. [Information obtained from reference 3.](#)

Magnetopause:

The magnetopause is a boundary layer that separates the magnetic field of the Earth from the magnetosheath. This region is located at approximately $10 R_{\oplus}$ on the side close to the sun, and extends to at least $80 R_{\oplus}$ on the antisolar side. The location can fluctuate by 1 to $3 R_{\oplus}$ and is known to expand or contract at rates larger than 50 km/sec during magnetic storms. The magnetopause is in the range of tens of km in thickness, and acts as a transition zone where the magnetic field direction shifts as much as 180° , and changes strength from more than 40 nT in the magnetosphere to 10 to 30 nT in the magnetosheath. [Information obtained from reference 3.](#)

Magnetotail:

The magnetotail is formed by the solar wind dragging the geomagnetic field lines away from the sun. The field lines of the magnetotail in the southern hemisphere are directed away from the Earth in the antisolar direction, while the field lines in the northern hemisphere point towards the sun. The magnetotail extends to a distance of at least $1000 R_{\oplus}$ from the Earth, and at $30 R_{\oplus}$ from the Earth in the antisolar direction, the radius is approximately $20 R_{\oplus}$. At locations from $8 R_{\oplus}$ to $10 R_{\oplus}$, the magnetic field intensity follows that of the Earth's dipolar field. At further distances, however, the field intensity decreases as the distance from the Earth increases. At $10 R_{\oplus}$ the field intensity is 20 nT, and at $80 R_{\oplus}$ the strength has decreased to about 7 nT. At $1000 R_{\oplus}$, the intensity has been observed to be between 4 and 16 nT. [Information obtained from reference 3.](#)

Neutral Sheet:

The neutral sheet separates the incoming and outgoing field lines in the magnetotail. In this region, the magnetic field intensity decreases to about 1 to 4 nT on the dawn meridian side, and to less than 1 nT on the side near the moon-midnight meridian plane. The neutral sheet extends from approximately $10 R_{\oplus}$ to the limit of the magnetotail, and is parallel with the solar-magnetospheric equatorial plane. Its position is above the plane during summer months, and below the plane during winter months. During magnetic storms, the neutral plane can be displaced beyond $13 R_{\oplus}$. The neutral sheet thickness ranges from 500 km to 5000 km. [Information obtained from reference 3.](#)

Cusp Region:

The cusp region is located on the antisolar side of the Earth and is the area where the geomagnetic field lines are first transformed into the magnetotail. This region occurs at a distance of 8 to $16 R_{\oplus}$ at geomagnetic latitudes of $\pm 25^{\circ}$. This region is part of the Van Allen radiation belts, and the outer boundary experiences sudden large changes in particle density. [Information obtained from reference 3.](#)

Origin of the magnetic field:

Origin of the magnetic field are discussed by Thompson⁴². The original thoughts on the origin of the geomagnetic field included ideas that the Earth acted as a large magnet. This idea started because of the large abundance of iron in the Earth's physical construction, but it is impossible for thermodynamic reasons. All physical materials lose their magnetism at high temperatures. Therefore, the magnetic moment of the material becomes randomly oriented, which cancels out the magnetization. Since the boundary of the Earth's core may be close to 3000° C and the Curie temperature of iron is not more than 780° C, the Earth cannot act as a magnet to produce the magnetic field. The other theory is: In the 1940's and 1950's, Elasser and Bullard⁵ claimed that: "the Earth's magnetic field arose from fluid motions in the dense metallic liquid core. This motion is caused by circulation of electric currents, and is able to run for a period of time due to self-induction. In order for this motion to occur, there must be a mechanism that controls and maintains the electric currents.

The self-exciting dynamo results from the interactions of the magnetic field with the flow of electric currents arising from fluid motion of the Earth's core. In the core, fluid motions across an existing magnetic field produce their own magnetic field and induced electric currents. The motion of the fluid, therefore, acts to reinforce and maintain the geomagnetic field by the way of a self-exciting dynamo."

The formulation of this dynamo theory is based on classical mechanics, thermodynamics, and electromagnetism. Solving the problem is difficult. The mathematical problems are nonlinear, and there are many physical unknowns and only a few observational constraints. Only a few solutions to simple similar problems exist. The magnetic field of the Earth is not a constant over time. Various changes occur in intensity and direction, including daily variations and ones due to the influence of the sun. [Information obtained from reference 3.](#)

Temporal Variations:

Temporal variations are described as disturbances in the geomagnetic field which result from changing positions of the Earth and the Sun. These variations usually only last for a short time, from a few seconds to a few days. [Information obtained from reference 3.](#)

The occurrence of the temporal variations is based on the rotation rates of the Earth and Sun. Every ~27 days, the Sun's rotation causes an active solar area to face the Earth. The magnitude of the temporal variations increases during the March-April and September-October times when the Earth is near the equinoxes. The intensity of the variations is linked to the number of sunspots. This number varies through an 11-year cycle. In addition, different types of temporal variations have effects on the intensity. [Information obtained from reference 3.](#)

Diurnal Variations:

Diurnal variations are one type of temporal variation. These variations occur in the day-to-night magnetic field intensity. The main causes of diurnal variations are changes in ionospheric currents resulting from systems of charged particles moving between 50 and 600 kilometers.

[Information obtained from reference 3.](#)

These effects are not prevalent in the geomagnetic field more than a few Earth radii away from the Earth's surface since the intensity of the magnetic fields resulting from the currents decreases with increasing distance.

Magnetic storms:

On occasion, plasma bursts emitted from solar flares cause the fairly constant solar wind to behave erratically. When the plasma comes in contact with the geomagnetic field, it causes it to become more compressed, and therefore raises the field intensity on the surface of the Earth. This occurrence is known as a magnetic storm. The initial phase of the magnetic storm lasts about one hour, and during this time, the total field intensity increases by about 50 nT. During very strong storms, the magnetopause can be compressed to below synchronous altitudes at this phase. The main phase of a magnetic storm can last for a few hours. During this time, the total field intensity decreases by more than 400 nT. The initial recovery phase lasts from six hours to two days, with final recovery to pre-storm levels lasting several days after that. During this time, a magnetic wave is formed, as shown in **Figure 1.7**.

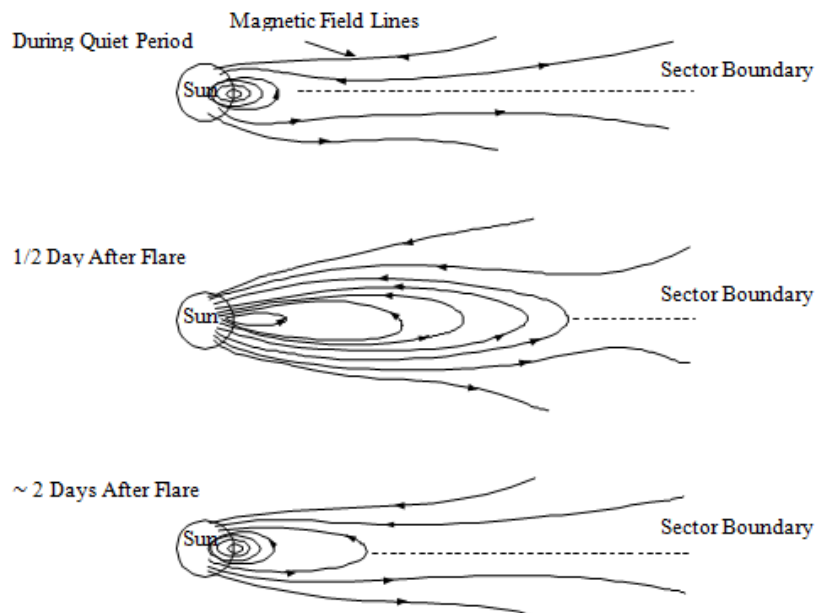


Figure 1.7: Appearance and Evolution of a Magnetic bottle (obtained from reference 5)

Secular Variations:

Unlike temporal variations, which are short-duration high-intensity variations, secular variations in the magnetic field occur gradually over very long periods of time. The secular variations are very small, but after a few years their accumulation is enough to make the magnetic field models outdated. Secular variation terms are estimated in magnetic field models to propagate data for a few years after the model epoch. The dipole strength of the magnetic field is decreasing by 0.05% per year. In addition, the portion of the dipole located in the Northern Hemisphere is drifting westward at 0.014 degrees per year. The changes in magnetic pole position in the North and South hemispheres are shown in **Figures 1.8** and **1.9** respectively. This drift implies that the possibility exists for a field reversal after a long period of time.

NORTH MAGNETIC POLE MOVEMENT

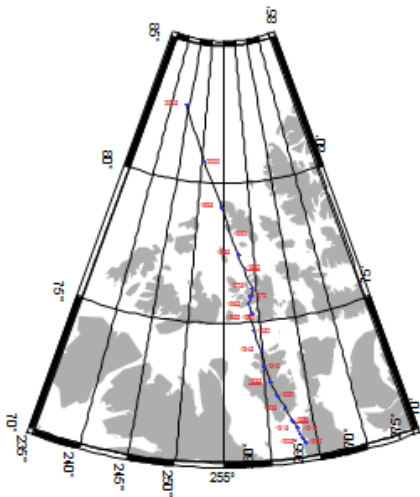


Figure 1.8: Movement of the North Pole over Time.

SOUTH MAGNETIC POLE MOVEMENT

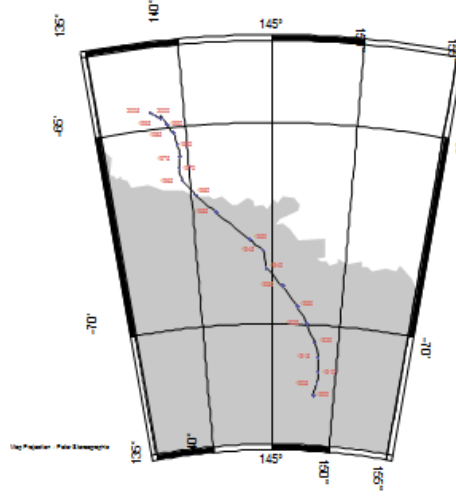


Figure 1.9: Movement of the South Pole over Time

Both Figures obtained from reference 6

Field Reversal:

The existence of field reversals has not been proven completely, but many arguments exist. Over the years, volcanic rocks have been discovered which are magnetized in the opposite direction to the geomagnetic field. Some scientists have argued that this magnetization was caused by a magnetic field reversal, while others insist that the rocks contained an internal mechanism that caused a spontaneous self-reversal.

As more rocks were discovered with this property, scientists noted that rocks of the same age at locations all around the world all had the same polarity, while no evidence for self-reversal could be located in the rocks. The current theory states that field reversals occur approximately every one or two million years, but this rate has varied over time. During the Cretaceous period, this was between 120 million and 80 million years before the present time, the reversals stopped, leaving the magnetic field in its normal polarity. Conversely, for 50 million years during the Permian period, 300 million years ago, the field remained in a reversed polarity.

Locating evidence for the transition fields that are expected to exist during magnetic field reversals, is difficult. Part of the reason for this is that the geomagnetic field has spent the majority of its time in either a stable normal or reversed state, or very little time in a mode of reversal. Therefore, the amount of rocks magnetized during this time is much less than those in the normal or reversed polarities. The currently accepted amount of time for the field to reverse is approximately 10^3 years.

1.2.3 Spacecraft magnetic field

Magnetic torques are prevalent in spacecraft. These torques can be in the form of magnetic disturbance torques which can alter the nominal motion of the spacecraft, or magnetic control torques which act to counteract the effects of the disturbance torques and change the orientation. The origin of magnetic torque can be examined by looking at the forces in a current carrying conductor. Current carrying loops produce magnetic torques, and a description of these torques follows. [Obtained from reference 7](#)

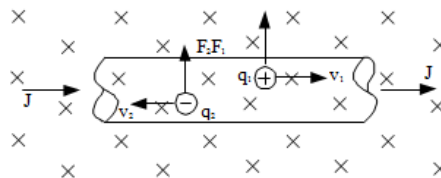


Figure 1.10: Forces on the Moving Charges in a Current-Carrying Conductor ([obtained from reference 8](#))

The force, ' \mathbf{F} ', on a current carrying conductor, such as a length of wire "Figure 1.10", is a summation of the forces on the moving charges:

$$(1.13) \quad \mathbf{F} = (n_1 \mathbf{A}_w l_w)(q_1 v_1 \mathbf{B}) + (n_2 \mathbf{A}_w l_w)(q_2 v_2 \mathbf{B})$$

Where a charge is represented by ' q_1 ', ' q_2 ', the drift velocity of the positive charge is ' v_1 ', ' v_2 ', and the number of positive charges is ' n_i ', where ' $i = 1$ ' for a positive charge, and ' $i = 2$ ' for a negative charge. The cross-sectional area of the wire is ' \mathbf{A}_w ' and ' l_w ' is the length. Since ' $(n_1 q_1 v_1 + n_2 q_2 v_2)$ ' is equal to the current density, ' \mathbf{J} ', and ' \mathbf{J} ' times ' \mathbf{A}_w ' is equal to the current, ' \mathbf{I} ', the force is:

$$(1.14) \quad \mathbf{F} = I l_w \mathbf{B}$$

This equation is only valid when the magnetic field is perpendicular to the wire. The component of the field which is parallel to the wire, ' \mathbf{B}_k ', exerts no force because it is in the same direction as the drift velocities. This relation leads to a general case force of:

$$(1.15) \quad \mathbf{F} = I l_w \mathbf{B} \sin \phi$$

Where ' ϕ ' is the angle between the ' \mathbf{B} ' field and the wire. In vector form this equation is written as:

$$(1.16) \quad \mathbf{F} = I l_w \times \mathbf{B}$$

For the general case.

Current loops:

When a current-carrying wire is arranged in a rectangular loop with sides ' \mathbf{a} ', ' \mathbf{b} ' and rotated an

angle ' α ' with respect to the magnetic field as shown in **Figure 1.11**:

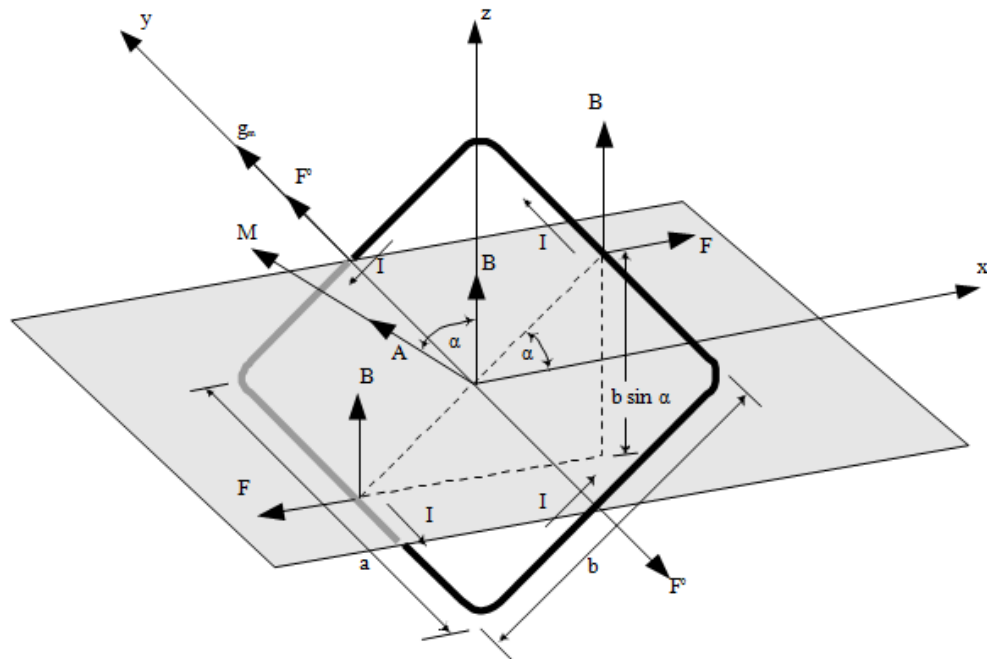


Figure 1.11: Forces on a Current-Carrying Loop in a Magnetic (obtained from reference 8)

The resultant force on the loop is zero. This resultant occurs because the forces on opposite sides of the loop are equal and opposite, and therefore cancel. A nonzero torque exists, however, arising from the fact that a moment couple is formed on sides a due to the angle ' α ' between the coil and magnetic field. This torque is equal to:

$$(1.17) \quad \mathbf{g}_m = IBA \sin \alpha$$

Where ' A ' is the area of the coil, ' a ' and ' b '. From this equation, it is evident that the magnetic torque is a maximum when ' $\alpha = 90^\circ$ ', and the plane of the coil is parallel to the magnetic field.

When

' $\alpha = 0^\circ$ ', the magnetic torque is equal to zero. In vector form, the torque is equal to:

$$(1.18) \quad \mathbf{g}_m = \mathbf{IA} \times \mathbf{B}$$

Here, 'A' is the area vector of the loop, or:

$$(1.19) \mathbf{A} = N\mathbf{A}\mu\hat{\mathbf{n}}$$

Where 'N' is the number of turns of wire, ' μ ' is the permeability of the core material, and ' $\hat{\mathbf{n}}$ ' is a unit vector normal to plane of the coil. The product of ' \mathbf{I} ' and ' \mathbf{A} ' is also known as the magnetic moment, or ' M '. The magnetic torque can therefore be described as:

$$(1.20) \mathbf{g}_m = M \times \mathbf{B}$$

The magnetic torque tends to rotate the loop towards an equilibrium position with ' M ' in the same direction as ' \mathbf{B} '.

Equations (1.13) – (1.20) obtained from reference 8.

Magnetic Disturbance Torques:

The main sources of magnetic disturbance torques arise from both internal and external magnetic activity. The spacecraft provides magnetic torques through permanent magnetism and spacecraft-generated current loops, while magnetism and currents induced by external fields also have an effect. Magnetic torques may also be a result of spacecraft assemblies that rotate relative to each other, such as rapidly spinning parts, or movable solar panels.

Magnetic disturbance torques must be given consideration in spacecraft and satellite design.

The main areas that need to be examined are attitude motion, control actuator sizing, expendable fuel requirements, and spin decay effects. Minimizing magnetic disturbance torques is important when the control torques are small, such as with gravity-gradient stabilization, or if long term small disturbances cause non-negligible effects, such as the precession of a spin stabilized spacecraft.

These disturbance torques do not cause a significant problem for attitude control, however, if the ambient field is negligibly small or if the spacecraft needs to be magnetically clean solely for the presence of magnetically sensitive equipment.

Effects:

Different sources of magnetic disturbance torques affect non-spinning and spinning spacecraft in various ways. In non-spinning spacecraft, permanent magnetism and spacecraft-generated current loops are a major source of torque. Magnetism induced by external fields causes the magnetic moment to vary depending on the intensity of the external field and characteristics of the magnetic material. There is no significant effect on non-spinning spacecraft by currents induced by a magnetic field.

In spinning spacecraft, only a portion of the torque from permanent magnetism and spacecraft-generated current loops are affected. In these current loops, the component of torque normal to the spin axis has a zero average value, and only the portion of dipole moment along the spin axis is considered. The magnetism induced by external fields causes the magnetic moment to vary depending on the external field as with the non-spinning spacecraft. It also causes spin decay due to magnetic hysteresis. Currents induced by external fields cause spin decay and precession by altering the spin-axis dipole moment.

Control of magnetic disturbances:

If a satellite is gravity-gradient stabilized, or if accurate control of the spin-axis of a spin stabilized spacecraft is required, the spacecraft magnetic dipole moment must be minimized such that it does not disturb the satellite orientation. Magnetic cleanliness for instruments onboard a spacecraft is obtained by reducing the magnetic field at a specific location on the spacecraft. The dipole moment of a spacecraft can be determined by exposing the satellite to a known, uniform magnetic field and determining the resulting torque. Once the dipole moment is known, curative procedures can be utilized to remove any necessary magnetization. One method of cancelling the effects of the spacecraft dipole moment is dumping, where residual magnetization is removed from major components and the entire spacecraft. Another method is compensation, in which small permanent magnets are attached to the spacecraft in order to minimize the dipole moment or magnetic field at a certain location.

Shielding components which produce large magnetic dipole moments by enclosing them in a container made from a highly permeable material is not a favorable action. The shielded product may have problems operating correctly, and therefore other means of reducing the dipole moment are preferred. [Above information obtained from reference 10](#)

Magnetic control torques:

Magnetic control torques can be applied to spacecraft to counteract disturbance torques or change the attitude. This counteraction is accomplished by applying a magnetic moment to the spacecraft by using current loops. The magnetic moment is in the form:

$$(1.21) \quad M = INA\mu\hat{n}$$

Where ' M ' is the magnetic moment, ' I ' is the current, ' N ' is the number of coils, ' A ' is the cross sectional area of the loop, ' μ ' is the permeability of the core material, and ' \hat{n} ' is a unit vector in the direction of the magnetic coil dipole.

As discussed previously, the magnetic torque acts in a direction orthogonal to both the magnetic field and the dipole moment. This interaction is illustrated in **Figure 1.12**.

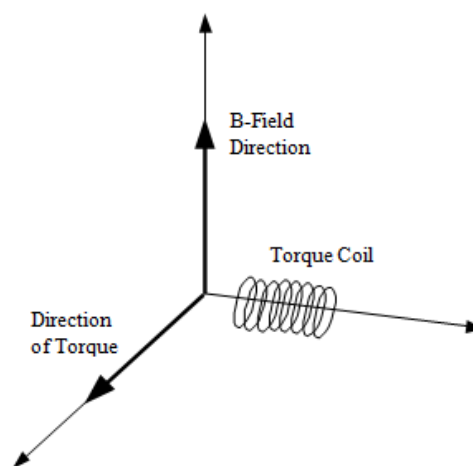


Figure 1.12: Magnetic Torque Direction [\(obtained from reference 11\)](#)

Often, the desired direction of torque is not perpendicular to the magnetic field. In this case, only the component of the desired torque in the direction perpendicular to the magnetic field is possible and can be developed. This relationship is demonstrated graphically in **Figure 1.13**:

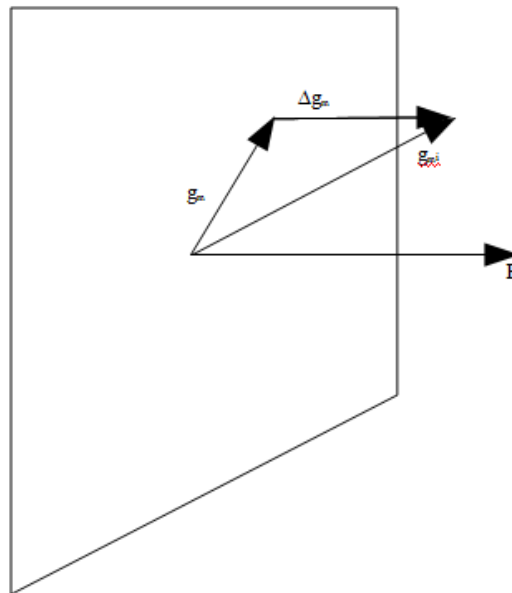


Figure 1.13: Magnetic control torque (obtained from reference 11)

The moment developed in a coil is determined by attempting to minimize the magnitude of the undesired magnetic torque, ' Δg_m ', such that:

$$(1.22) \quad \|g_m - g_{m_i}\| = \text{minimum}$$

That goes to:

$$(1.23) \quad \Delta g_m = (g_{m_i} \cdot \hat{B})\hat{B}$$

' \hat{B} ' is a unit vector in the direction of the magnetic field, from vector addition:

$$(1.24) \mathbf{g}_m = \mathbf{g}_{m_i} - \Delta \mathbf{g}_m$$

Once the actual applicable torque is known, the magnetic moment that should be developed can be calculated with equation:

$$(1.25) M = (\mathbf{B} \times \mathbf{g}_m) / B^2$$

Equations (1.21) – (1.25) obtained from reference 11

Magnetic Control Hardware:

Torque coils

Torque Coils consist of loops of a conducting wire, such as copper, around an air core. They work by providing a magnetic moment, which interacts with the magnetic field to produce a torque, as in the current loops of previous section. The magnetic moment of the coil is defined from **(1.21)**. For an air core loop, the value for the permeability of the core material, ' μ ', is equal to 1.

Torque rods

Torque rods work under the same principal as torque coils. The main difference between torque coils and torque rods is the core material and thus the values of ' μ ' are different. Whereas torque coils have air in their core, torque rods have cores of metal. The core material choice is important for the torque rods. Ferromagnetic materials are often used because they have high permeability's which can lead to a reduction in power consumption. However, ferromagnetic materials saturate at low values of magnetic field intensity. In addition, their permeability is a function of the magnitude of the magnetic field intensity, and therefore the dipole moment is difficult to predict.

Obtained from reference 12

Permanent magnets

Florin describes a technique of using a system of gimbaled permanent magnets for magnetic control. A gimbal is used to position two permanent magnets so a magnetic moment can be induced in any direction. The strength of the magnetic moment created ranges from zero to twice that of one magnet. [Obtained from reference 13](#)

Magnetic Field and Orbit Interaction

Since the magnetic control torque on a spacecraft can only act perpendicular to the magnetic field, the direction of the magnetic field over the duration of an orbit is important to determine.

Equatorial Orbits

If it is assumed that the magnetic field axis is coincident with the spin axis, the magnetic field direction around the equator is nearly parallel with the angular momentum direction of the Earth, as shown in **Figure 1.14**. In an equatorial orbit, therefore, the pitch direction, or $\hat{2}'$, is always in the same direction as the magnetic field. For this reason, no magnetic control in the pitch direction is possible in equatorial orbits.

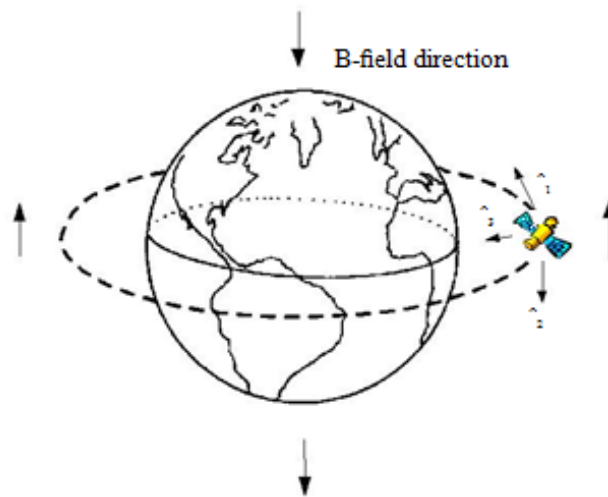


Figure 1.14: Equatorial Orbit in Magnetic field

Polar Orbits

Once again assuming that the magnetic field axis is coincident with the spin axis, the controllability of a polar orbit can be examined. As the spacecraft passes over the equator, the magnetic field is aligned with the roll direction, or $\hat{1}'$, as shown in **Figure 1.15**, and no roll control is possible. As the distance from the equator increases, the amount of roll control possible increases but the amount of yaw control decreases. When the spacecraft is over the poles, the magnetic field is in the same direction as the yaw vector, $\hat{3}'$. Therefore no magnetic yaw control is possible in these locations.

Circular Orbits

For circular orbits that are neither equatorial nor polar, the controllability varies depending on the position in the orbit. One thing that does remain nearly constant is the magnitude of the magnetic field component in the \hat{z} direction.

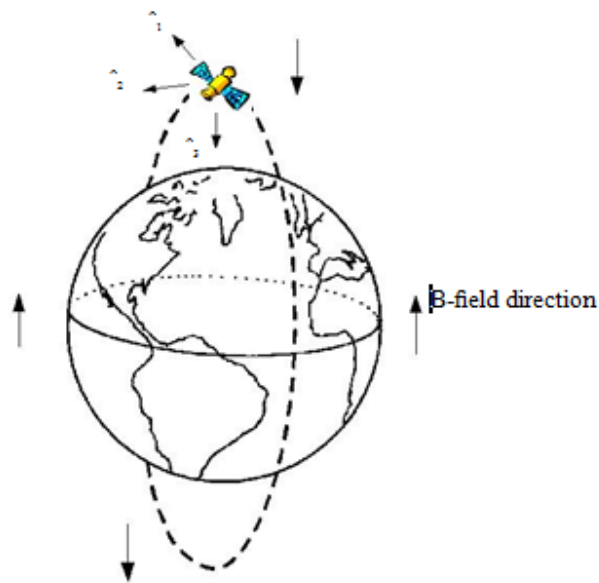


Figure 1.15: polar orbit in Magnetic Field

1.2.4 Literature review discussion

Knowledge of the structure of magnetic field is very vital for this project. To be able to determine the position of the satellite and to control it using magnetic coils. The information provided in literature overview thoroughly explained how the magnetic field formed and how the satellite magnetic field react to respect earth's magnetic field.

First chapter provided the information of the magnetic field in general, its origin and specifications. Next chapter went to earth magnetic field, where different areas of geomagnetic fields are presented also different anomalies. The third chapter is about satellite magnetic interactions with earth magnetic field, where the different types of torques discussed and the different types of hardware to control those torques.

CHAPTER 2

ADAC SYSTEM

Attitude determination and control system (ADAC), is a system designed to determine position of the satellite in space and to make control, of above satellite, to be possible. ADAC system is a combination of the Spacecraft dynamics that include understanding of Orbit dynamics, coordinate system and attitude dynamics as well as control system methods.

2.1 Dynamics and Attitude determination

2.1.1 Spacecraft and orbit dynamics

The way that a spacecraft moves is described using orbit dynamics, which determines the position of the body, as well as attitude dynamics, which determines the orientation. This chapter develops equations describing both orbit and attitude dynamics. In addition, frames of reference and attitude rotations are discussed, along with environmental disturbance torques. This chapter concludes with information on attitude determination and control methods.

Orbit Dynamics:

Orbit dynamics determine the position of a body orbiting another body. It is applicable for spacecraft orbiting planets, as well as for planets, such as the Earth, orbiting the Sun. Orbit dynamics are described by Bate, Mueller, and White. [Obtained from reference 14](#)

Keplerian orbits:

In 1609, Johann Kepler discovered that heavenly bodies orbit in elliptical paths.

He determined three laws which describe all planetary motion.

Kepler's laws:

1. The orbit of each planet is an ellipse, with the Sun at a focus.
2. The line joining the planet to the Sun sweeps out equal areas in equal times.

3. The square of the period of a planet is proportional to the cube of its mean distance from the Sun.

Obtained from reference 14

All bodies are under the influence of Newton's Laws. In particular, Newton's Second Law states that the rate of change of momentum is proportional to the force impressed and is in the same direction as that force, or:

$$(2.1) \quad \sum \mathbf{F} = m\ddot{\mathbf{r}}$$

Where ' $\sum \mathbf{F}$ ' is the vector sum of the forces acting on mass ' m ', and ' $\ddot{\mathbf{r}}$ ' is the vector acceleration of ' m ' relative to an inertial reference frame. In addition, Newton formulated his Law of Universal Gravitation. This law states that any two bodies attract one another with a force proportional to their masses and inversely proportional to the square of the distance between them, or:

$$(2.2) \quad \mathbf{F} = -\frac{GMm}{r^2} \frac{\mathbf{r}}{r}$$

where ' \mathbf{F} ' is the force on mass m due to mass ' M ', ' \mathbf{r} ' is the vector from ' M ' to ' m ', and ' G ' is the universal gravitational constant with a value of $6.670 \times 10^{-11} \text{m}^3/(\text{kg}\cdot\text{s}^2)$. When examining the relative motion of two bodies, such as the orbit of a planet around the Sun, or a satellite around a planet, it is convenient to consider the two-body problem. Two assumptions are made to simplify the problem. One is that the bodies are spherically symmetric, and can be modeled with the masses concentrated at the center of the body. The second assumption declares that there are no external or internal forces acting on the system other than the force of the gravitational attractions.

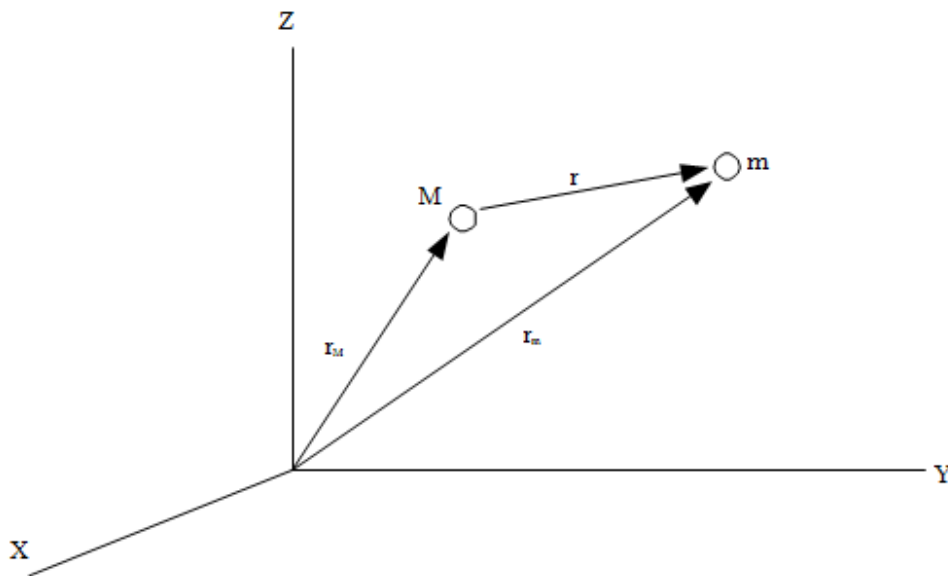


Figure 2.1: Relative Motion of Two Bodies (obtained from reference 14)

The relative motion of two bodies is shown in **Figure 2.1**. The vector ' \mathbf{r} ' is defined as:

$$(2.3) \quad \mathbf{r} = \mathbf{r}_m - \mathbf{r}_M$$

Applying Newton's laws to the system gives:

$$(2.4) \quad m\ddot{\mathbf{r}}_m = -\frac{GMm}{r^2} \frac{\mathbf{r}}{r}$$

$$(2.5) \quad M\ddot{\mathbf{r}}_M = \frac{GMm}{r^2} \frac{\mathbf{r}}{r}$$

Which leads to:

$$(2.6) \quad \ddot{\mathbf{r}}_m = -\frac{GM}{r^3} \mathbf{r}$$

$$(2.7) \quad \ddot{\mathbf{r}}_{\mathbf{M}} = -\frac{G\mathbf{m}}{r^3}\mathbf{r}$$

Subtracting (2.7) from (2.6):

$$(2.8) \quad \ddot{\mathbf{r}} = -\frac{G(\mathbf{M}+\mathbf{m})}{r^3}\mathbf{r}$$

For the application of the interaction of a satellite and a planet, the mass of the satellite, ' \mathbf{m} ', is much less than the mass of the planet, ' \mathbf{M} '. Therefore:

$$(2.9) \quad G(\mathbf{M} + \mathbf{m}) \approx G\mathbf{M}$$

The gravitational parameter, ' μ ', is defined as:

$$(2.10) \quad \mu \equiv G\mathbf{M}$$

For the Earth, this value is equal to:

$$(2.11) \quad \mu_{\oplus} = 3.986032 \times 10^5 \frac{km^3}{sec^2}$$

With the approximation:

$$(2.12) \quad \ddot{\mathbf{r}} + \frac{\mu}{r^3}\mathbf{r} = 0$$

Where ' \mathbf{r} ' is the position vector of the second body with respect to the first.

Angular momentum:

Angular momentum, ' \mathbf{h} ', is a constant of motion because it is a central force. A force tangential to the center of rotation must be applied to change the angular momentum of a rotational motion

system. Since the gravitational force is always directed inward towards the center of mass, the angular momentum of the spacecraft around the center of mass does not change. The specific angular momentum is defined as:

$$(2.13) \quad \mathbf{h} = \mathbf{r} \times \mathbf{v}$$

The directions of ' \mathbf{r} ' and ' \mathbf{v} ' must remain in the plane of the orbit in order for the angular velocity to be constant. The magnitude of the angular velocity is:

$$(2.14) \quad h = r v \cos \phi_f$$

Where ' ϕ_f ': is the flight path angle, or the angle between the local horizontal and the velocity vector direction.

Orbit equations:

Although the majority of satellites follow elliptical or circular orbits, these are not the only paths satisfied by equation (2.12). Any curve defined by a conic section is a valid orbit. The type of curve is determined by examining the polar equation of a conic section:

$$(2.15) \quad r = \frac{p}{1 + e \cos v}$$

Where ' v ' is the polar angle between ' \mathbf{r} ' and the point on the orbit closest to the focus, and ' p ' is the semilatus parameter. These values are shown in **Figure 2.2**. The value of the eccentricity, ' e ' determines the shape of the orbit as detailed below:

$e = 0$	circle
$0 < e < 1$	ellipse
$e = 1$	parabola
$e > 1$	hyperbola

Figure 2.2: value of eccentricity

The orbits discussed in this report are elliptical, and therefore the eccentricity is constrained as $0 \leq e < 1$. The period of the orbit is equal to:

$$(2.16) \quad T = \frac{2\pi}{\sqrt{\mu}} a^{3/2}$$

Where 'a' the semi-major axis. This agrees with Kepler's third law which states that the square of the period is proportional to the cube of the mean distance.

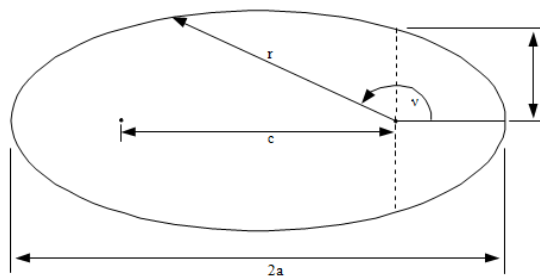


Figure 2.2: Elliptical Orbit

Orbital Elements:

The orbit of a satellite can be described by five numbers, known as orbital elements. A sixth orbital element is added to determine the location of the satellite along the orbit. The orbital elements are shown in **Figure 2.3**:

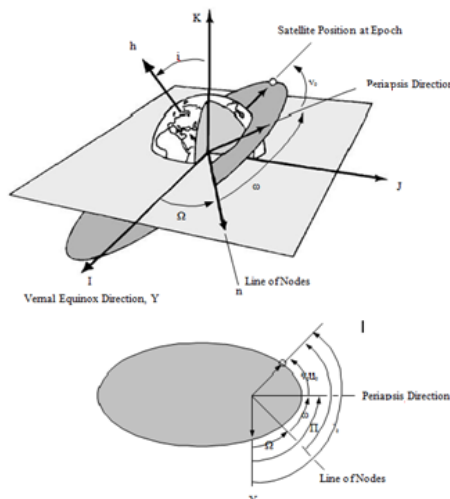


Figure 2.4: Orbital Elements (obtained from reference 14)

The first two elements describe the shape of the orbit.

1. ' a ', semi-major axis - a constant defining the size of the orbit
2. ' e ', eccentricity - a constant defining the shape of the orbit

The next two elements describe the position of the plane of the orbit.

3. ' i ', inclination - angle between the ' K ' axis and the angular momentum vector, ' h '
4. ' Ω ', right ascension of the ascending node - the angle in the fundamental plane, between the ' I ' axis and the point where the satellite crosses the fundamental plane in an ascending direction measured counterclockwise when viewed from North of the fundamental plane.

The fifth element describes the rotation of the elliptical orbit in its plane.

5. ' ω ', argument of periapsis - the angle, in the plane of the satellite's orbit, between the ascending node and the periapsis point, measured in the direction of the satellite's motion.

The sixth element describes the position of the satellite in the orbit.

6. ' T ', time of periapsis passage - time when the satellite was at periapsis

While the above six orbital elements are classically used to describe the position of a satellite, they are not exclusive. Instead of the argument of periapsis, the longitude of periapsis, ' Π ', is occasionally used. This is the angle from the ' I ' direction to periapsis measured eastward. The time of periapsis passage, ' T ', can be replaced with the true anomaly at epoch, ν_0 , which is the angle in the plane of the satellite's orbit between periapsis and the position of the satellite at a particular epoch, ' t_0 '. Additionally, the argument of latitude at epoch, ' u_0 ' can be used. This is the angle in the plane of the orbit between the ascending node and the radius vector of the satellite at epoch. These values are related by:

Obtained from reference 14

$$(2.17) \quad u_0 = \omega + \nu_0$$

The true longitude at epoch, l_0 may also be used to describe the position of the satellite.

This angle is measured eastward from the ' I ' axis to the ascending node, and then in the orbital plane to the radius direction at epoch. This relation is defined as:

$$(2.18) \quad l_0 = \Omega + \omega + \nu_0 = \Pi + \nu_0 = \Omega + \mathbf{u}_0$$

Certain orbits cause some of the orbital elements to be undefined. When the orbit is circular, there is no periapsis, and ' ω ', ' Π ', and ' ν_0 ' are undefined. When the orbit is equatorial, there is no ascending node and therefore ' ω ' and ' \mathbf{u}_0 ' are undefined. In these cases, using ' l_0 ' instead of ' ω ' is useful.

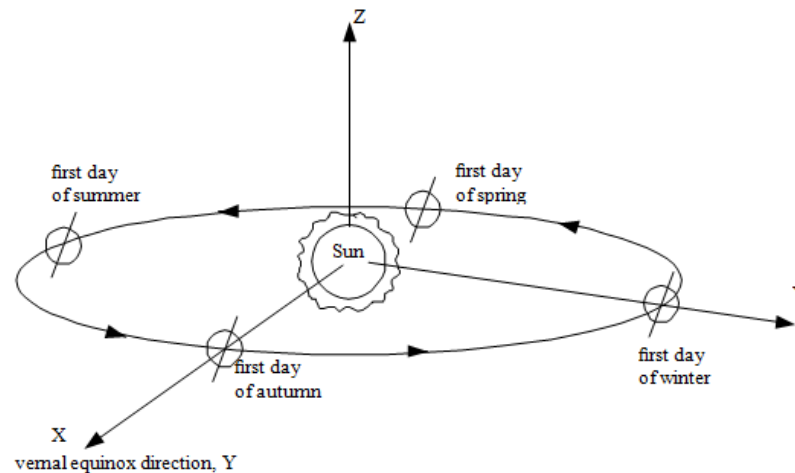


Figure 2.4: Heliocentric-Ecliptic Coordinate System (obtained from reference 14)

Coordinate systems:

When describing orbital motion, it is necessary to reveal which coordinate system is used. The coordinate systems must be inertial such that the frame is fixed to an outside observer.

A fixed coordinate system may also be used to describe satellite motion, but a rotation between the inertial and Earth-fixed coordinate systems must be incorporated into the definition.

Heliocentric-Ecliptic:

Bodies that orbit around the Sun, such as the Earth and other planets as well as interplanetary space vehicles, are typically described in the Heliocentric-ecliptic frame of reference shown in **Figure 2.4**. This reference frame is inertial, with the **Z** direction perpendicular to the plane of the ecliptic, which is the plane of the Earth's revolution around the Sun. The direction of the **X** axis is in the vernal equinox direction, and the **Y** direction is orthogonal.

Earth-centered Inertia:

The Earth-Centered Inertial (ECI) coordinate system is centered in the middle of the Earth, as shown in **Figure 2.5**. The **Z** axis points through the geographic North Pole, or the axis of rotation. The **X** axis is in the direction of the vernal equinox, and the **Y** direction is orthogonal. The Earth rotates with respect to the ECI coordinate frame.

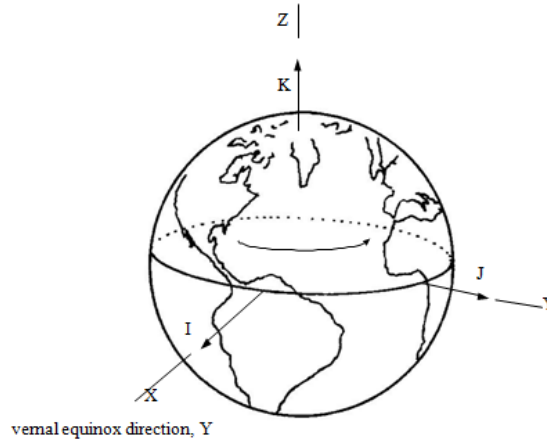


Figure 2.5: Earth-Centered Inertial reference Frame (obtained from reference 14)

Earth-centered Earth-Fixed:

The Earth-centered Earth-fixed (ECEF) reference frame also has its origin at the center of the Earth, but it rotates relative to inertial space, shown in **Figure 2.6**. The '**K**' axis is through the North Pole, and the '**I**' axis points to the Greenwich Meridian. The angle between the vernal equinox direction and the Greenwich Meridian must be defined. This is known as the Greenwich sidereal time, ' **θ_g** '. Greenwich sidereal time is documented at various epochs and can be extracted from data tables as 0. At any time after epoch, ' **θ_g** ' can be determined from ' **θ_{g_0}** ' by:

$$(2.19) \quad \theta_g = \theta_{g_0} + \omega_{\oplus}(t - t_0)$$

Where ' **ω_{\oplus}** ' is the angular velocity of the Earth. On January 1, 2000 at midnight, the value of ' **θ_{g_0}** ' was equal to **6h 39m 52.2707s**, or **99.96779°** according to the Multiyear Interactive Computer Almanac from the U.S. Naval Observatory. Obtained from reference 15

This value changes slightly from year to year, and on January 1, 2001 was equal to **6h 42h 51.5354s**, or **100.71473°**

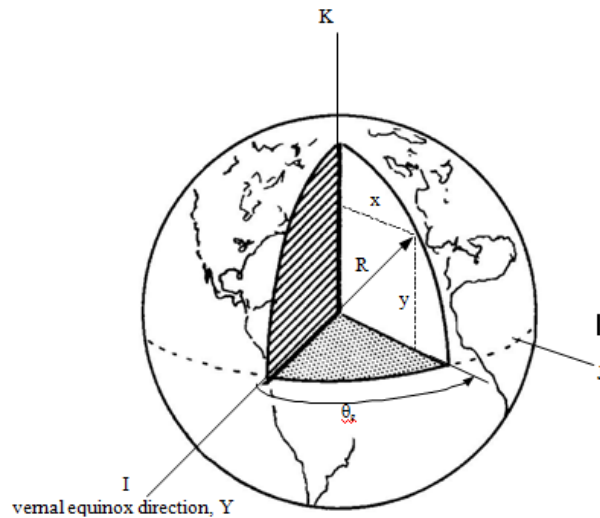


Figure 2.6: Earth-Centered Earth-Fixed Reference Frame (obtained from reference 14)

Equations (2.1) – (2.19) were obtained from reference 14

2.1.2 Attitude Dynamics

Attitude dynamics describe the orientation of a body in an orbit and can be explained using rotations. When examining attitude dynamics, it is important to describe the reference frames being used to give a basis for the rotations.

Reference Frames

Three main reference frames are used to describe the orientation, or attitude, of a spacecraft in orbit. These are the inertial, orbital, and body frames.

Inertial frame:

An inertial frame is used for attitude applications. The **X** direction points from the focus of the orbit to the vernal equinox, **Y**, the **Z** direction is in the orbital angular velocity direction, and **Y** is perpendicular to **X** and **Z**.

Orbital frame:

The orbital frame is located at the mass center of the spacecraft, and the motion of the frame depends on the orbit. This frame is non-inertial because of orbital acceleration and the rotation of the frame. The \hat{z} axis is in the direction from the spacecraft to the Earth, \hat{y} is the direction opposite to the orbit normal, and \hat{x} is perpendicular to \hat{y} and \hat{z} . In circular orbits, \hat{x} is the direction of the spacecraft velocity. The three directions \hat{x} , \hat{y} , and \hat{z} are also known as the roll, pitch, and yaw axes, respectively. **Figure 2.7**, shows a comparison of the inertial and orbital frames in an equatorial orbit.

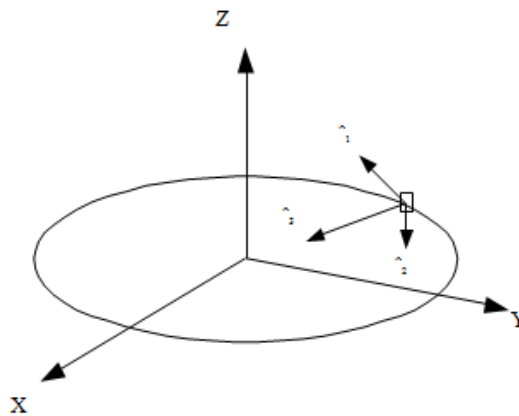


Figure 2.7: Earth-Centered Inertial and Orbital Reference Frames (obtained from reference 14)

Body Frame:

Like the orbital frame, the body frame has its origin at the spacecraft's mass center. This frame is fixed in the body, and therefore is non-inertial. The relative orientation between the orbital and body frames is the basis of attitude dynamics and control.

Principal Axis:

Like the orbital frame, the body frame has its origin at the spacecraft's mass center. This frame is fixed in the body, and therefore is non-inertial. The relative orientation between the orbital and body frames is the basis of attitude dynamics and control.

Rotations

Rotations and transformations are performed to obtain the desired vector in alternate reference frames. Two notations commonly used to describe this rotation are Euler angles and quaternions.

Rotations are discussed by Hall. [Obtained from reference 16](#)

Rotation Matrix:

The relationship between vectors expressed in different reference frames is described as:

$$(2.20) \quad \mathbf{v}_i = R^{ib} \mathbf{v}_b$$

Where $'R^{ib}'$ is the rotation from $'\mathbf{F}_b'$ to $'\mathbf{F}_i'$, \mathbf{v}_i is a vector in $'\mathbf{F}_i'$, and \mathbf{v}_b is the same vector in $'\mathbf{F}_b'$.

The components of a rotation matrix are the direction cosines of the two sets of reference axes. In general,

$$(2.21) \quad \mathbf{R}^{21} = \begin{bmatrix} \cos \theta_{x_2x_1} & \cos \theta_{x_2y_1} & \cos \theta_{x_2z_1} \\ \cos \theta_{y_2x_1} & \cos \theta_{y_2y_1} & \cos \theta_{y_2z_1} \\ \cos \theta_{z_2x_1} & \cos \theta_{z_2y_1} & \cos \theta_{z_2z_1} \end{bmatrix}$$

Where $'\cos \theta_{x_1x_2}'$ is the cosine of the angle between the \mathbf{x} axis of the first frame and the \mathbf{x} axis of the second frame. The rotation matrix from the inertial reference frame to the orbital reference frame is defined

$$(2.22) \quad \mathbf{R}^{oi} = \begin{bmatrix} -\sin u \cos \Omega - \cos u \cos i \sin \Omega & -\sin u \sin \Omega + \cos u \cos i \cos \Omega & \cos u \sin i \\ -\sin i \sin \Omega & \sin i \cos \Omega & -\cos i \\ -\cos u \cos \Omega + \sin u \cos i \sin \Omega & -\cos u \sin \Omega - \sin u \cos i \cos \Omega & -\sin u \sin i \end{bmatrix}$$

Which is a rotation, based on the orbital elements.

Quaternions:

A second way to express a rotation is through the use of quaternions. The quaternion set, $'\tilde{\mathbf{q}}'$, is a 4×1 matrix consisting of a vector portion, \mathbf{q} and a scalar portion, q_4 .

$$(2.23) \quad \tilde{\mathbf{q}} = [\mathbf{q}^T \ q_4]^T$$

The rotation matrix in terms of the quaternion is:

$$(2.24) \quad \mathbf{R} = (q_4^2 - \mathbf{q}^T \mathbf{q})\mathbf{1} + 2\mathbf{q}\mathbf{q}^T - 2q_4\mathbf{q}^\times$$

Where ' \mathbf{q}^\times ' is the skew symmetric of ' \mathbf{q} ' defined as:

$$(2.25) \quad \mathbf{q}^\times = \begin{bmatrix} 0 & -q_3 & q_2 \\ q_3 & 0 & -q_1 \\ -q_2 & q_1 & 0 \end{bmatrix}$$

In addition, ' $\tilde{\mathbf{q}}$ ' can be expressed in terms of ' \mathbf{R} ' as:

$$(2.26) \quad \begin{aligned} q_4 &= \pm \frac{1}{2} \sqrt{1 + \text{trace } \mathbf{R}} \\ \mathbf{q} &= \frac{1}{4q_4} \begin{bmatrix} R_{23} - R_{32} \\ R_{31} - R_{13} \\ R_{12} - R_{21} \end{bmatrix} \end{aligned}$$

Quaternions have advantages and disadvantages over rotation matrix notation. The singularities that exist when certain Euler angles are small are eliminated with the use of quaternions. However, the physical meaning of quaternions is obscure and not as intuitive as rotation angles.

Angular velocity:

The angular velocity, ' $\boldsymbol{\omega}$ ', is used to examine the angular displacements that occur over time.

Angular velocities are dependent on the frame of reference, and are designated by ' $\boldsymbol{\omega}_b^{ca}$ ', which is a rotation of ' \mathbf{F}_c ' with respect to ' \mathbf{F}_a ' as seen by ' \mathbf{F}_b '

Angular velocities add, but only when they are in the same reference frame. For example, the following relation is valid:

$$(2.27) \quad \omega_b^{bi} = \omega_b^{bo} + \omega_b^{oi}$$

When the angular velocities are in different reference frames, however, it is necessary to perform rotations. This is evident in:

$$(2.28) \quad \omega_b^{bi} = R^{bo} \omega_b^{bo} + R^{bi} \omega_b^{oi}$$

Where the angular velocity is seen by the body frame.

Equation of motion

Equation of motion, is a derivation of equations of motion for a satellite system.

Dynamic equation of motion:

The Rotational equations for a rigid body are derived by beginning with the rotational equivalent of:

$$(2.29) \quad m\vec{a} = \vec{f}$$

Or

$$(2.30) \quad \dot{\vec{h}} = \vec{g}$$

Where \vec{h} the angular momentum about the mass center, and \vec{g} is the torque. This relationship is represented in matrix form by:

$$(2.31) \quad \dot{\vec{h}} + \omega_b^{bi} \times \vec{h}$$

Assuming that the body frame is fixed to the body at the mass center, the angular momentum can be represented by:

$$(2.32) \quad \mathbf{h} = \mathbf{I}\boldsymbol{\omega}_b^{bi}$$

Which leads to:

$$(2.33) \quad \mathbf{I}\dot{\boldsymbol{\omega}}_b^{bi} + \boldsymbol{\omega}_b^{bi} \times \mathbf{I}\boldsymbol{\omega}_b^{bi} = \mathbf{g}$$

Solving for $\mathbf{I}\dot{\boldsymbol{\omega}}_b^{bi}$ leads to:

$$(2.34) \quad \dot{\boldsymbol{\omega}}_b^{bi} = -\mathbf{I}^{-1}\boldsymbol{\omega}_b^{bi} \times \mathbf{I}\boldsymbol{\omega}_b^{bi} + \mathbf{I}^{-1}\mathbf{g}$$

In this study, the only torques, ' \mathbf{g}' ' are gravity-gradient and magnetic is expanded into:

$$(2.35) \quad \dot{\boldsymbol{\omega}}_b^{bi} = \begin{bmatrix} \frac{I_2 - I_3}{I_1} \omega_2 \omega_3 + \frac{g_1}{I_1} \\ \frac{I_3 - I_1}{I_2} \omega_3 \omega_1 + \frac{g_2}{I_2} \\ \frac{I_1 - I_2}{I_3} \omega_1 \omega_2 + \frac{g_3}{I_3} \end{bmatrix}$$

If principle axes are used, these equations are known as Euler's Equations.

Kinematic Equations of motion:

The kinematic equations of motion are obtained by beginning with the definition of a quaternion.

The quaternion is in the form:

$$(2.36) \quad \bar{\mathbf{q}} = \begin{bmatrix} a \sin \frac{\Phi}{2} \\ \cos \frac{\Phi}{2} \end{bmatrix}$$

Where ' \mathbf{a}' ', is the Euler axis vector and ' Φ ' is the angle of rotation. At time ' $(t + \Delta t)$ ' the quaternion

is equal to:

$$(2.37) \quad \bar{\mathbf{q}}(t + \Delta t) = \left(\cos \frac{\Delta\Phi}{2} \mathbf{1} + \sin \frac{\Delta\Phi}{2} \begin{bmatrix} 0 & a_3 & -a_2 & a_1 \\ -a_3 & 0 & a_1 & a_2 \\ a_2 & -a_1 & 0 & a_3 \\ -a_1 & -a_2 & -a_3 & 0 \end{bmatrix} \right) \bar{\mathbf{q}}(t)$$

Since ' Δt ' is infinitesimal and ' $\Delta\Phi = \omega\Delta t$ ', where ' ω ' is the magnitude of the instantaneous angular velocity of the body, the following small angle assumptions are used:

$$(2.38) \quad \cos \frac{\Delta\Phi}{2} \approx 1 \quad \sin \frac{\Delta\Phi}{2} \approx \frac{1}{2}\omega\Delta t$$

This leads to:

$$(2.39) \quad \bar{\mathbf{q}}(t + \Delta t) = \left[\mathbf{1} + \frac{1}{2}\boldsymbol{\Omega}\Delta t \right] \bar{\mathbf{q}}(t)$$

Where ' $\boldsymbol{\Omega}$ ' is the skew symmetric matrix:

$$(2.40) \quad \boldsymbol{\Omega} = \begin{bmatrix} 0 & \omega_3 & -\omega_2 & \omega_1 \\ -\omega_3 & 0 & \omega_1 & \omega_2 \\ \omega_2 & -\omega_1 & 0 & \omega_3 \\ -\omega_1 & -\omega_2 & -\omega_3 & 0 \end{bmatrix}$$

The derivative of the quaternion is:

$$(2.41) \quad \dot{\bar{\mathbf{q}}} = \lim_{\Delta t \rightarrow 0} \frac{\bar{\mathbf{q}}(t + \Delta t) - \bar{\mathbf{q}}(t)}{\Delta t} = \frac{1}{2}\boldsymbol{\Omega}\bar{\mathbf{q}}$$

This is rearranged as:

$$(2.42) \quad \dot{\mathbf{q}} = \frac{1}{2} \begin{bmatrix} q_4 & -q_3 & q_2 \\ q_3 & q_4 & -q_1 \\ -q_2 & q_1 & q_4 \\ -q_1 & -q_2 & -q_3 \end{bmatrix} \begin{bmatrix} \omega_1 \\ \omega_2 \\ \omega_3 \end{bmatrix} = \frac{1}{2} \begin{bmatrix} \mathbf{q}^\times + q_4 \mathbf{1} \\ -\mathbf{q}^T \end{bmatrix} \boldsymbol{\omega}$$

This equation represents the kinematic equation of motion of the spacecraft.

Equations (2.20) – (2.42) obtained from reference 16

2.1.3 Attitude determination

The orientation of a spacecraft can be determined by describing the rotation between a spacecraft fixed reference frame and a known reference frame. This description is accomplished by finding rotations between measured attitude vectors and known quantities. For example, a Sun sensor determines the vector from the spacecraft to the Sun in the body frame, ' \mathbf{s}_b '. Since the vector in the inertial frame, ' \mathbf{s}_i ', can be calculated from ephemeris data, the following relation is useful:

$$(2.43) \quad \mathbf{s}_b = \mathbf{R}^{bi} \mathbf{s}_i$$

The attitude is determined by solving for ' \mathbf{R}^{bi} '. This equation does not have a unique solution, however, so it is necessary to obtain a second attitude measurement to fully describe the attitude of a spacecraft.

Common attitude sensors include Sun sensors, Earth sensors, magnetometers, star trackers, and gyroscopes, and are described by Wertz and Larson. Obtained from reference 17

A comparison of the ranges of these attitude sensors is shown in **Figure 2.9**:

Sensor	Accuracy	Characteristics and Applicability
Magnetometers	1.0° (5,000 km alt) 5° (200 km alt)	Attitude measured relative to Earth's local magnetic field. Magnetic field uncertainties and variability dominate accuracy. Usable only below ~6,000 km.
Earth Sensors	0.05° (GEO) 0.1° (low altitude)	Horizon Uncertainties dominate accuracy. Highly accurate units use scanning.
Sun Sensors	0.01°	Typical field of view ±130°
Star Sensors	2 arc sec	Typical field of view ±16°
Gyroscopes	0.001°/hour	Normal use involves periodically resetting the reference position.

Figure 2.8: Ranges of sensor Accuracy (obtained from reference 17)

Magnetometers:

Magnetometers measure the strength and direction of the Earth's magnetic field to determine the orientation of a spacecraft with respect to the local magnetic field. Magnetometers are often inexpensive and have low power requirements. In addition, the magnetic field can always be measured in low Earth orbits. Magnetometers have some disadvantages, too. They often have poor resolution and do not give good results if they are far from the Earth. The measurements are limited by the strength of the local field strength, as well as the accuracy of the magnetic field model.

Earth sensor:

The Earth can be detected for attitude determination by examining the location of the horizon. Most Earth sensors use a spinning motion that can scan for the horizon line. Detecting the Earth has advantages because it is bright and not easily confused with other bodies. It has disadvantages including a resolution of only 0.1° due to an uncertainty in the horizon. Also, if a scanning motion is required, the sensors can be complicated.

Sun Sensors:

Sun sensors are one of the most common attitude determination sensors because the Sun is easy to detect. It is bright and not easily confused with other bodies. Sun sensors have low power requirements. However, the Sun is not always visible. In addition, the accuracy is limited since the angular diameter of the Sun as seen from the Earth is approximately $1/2^\circ$.

2.2 Control of satellite

Some form of attitude control is required to change the attitude of a spacecraft or keep it in a stable position. Three main types of control are often used. These types of control include spin stabilization, three-axis control techniques, and passive control.

2.2.1 Control and stabilization

Three -axis stabilization:

Some spacecraft require autonomous control of all three axes during their missions. Three- axis control systems include wheels, magnetic control devices, and thrusters. Advantages to these systems include good pointing accuracy, and a non-inertial pointing accuracy. However, the hardware is often expensive, and complicated, leading to a higher weight and power.

Passive Control:

Passive control techniques can be used for attitude control. These can be advantageous because they do not require moving parts, and therefore there is a savings on mass, power, and cost. In addition, they have the possibility for long lifetimes. However, there is a poor pointing accuracy that can be obtained. The most common passive control is gravity gradient, but a passive magnetic system is also possible.

Passive Magnetic:

Another type of passive stabilization uses permanent magnets. The magnets force alignment along the Earth's magnetic field lines. This stabilization is most effective in near equatorial orbits since the magnetic field orientation is almost constant. This method can only be used in orbits close to the Earth, and only when the mission allows the orientation of the spacecraft to vary with the magnetic field.

2.2.2 Control laws

Magnetic control laws are derived to stabilize a spacecraft. Both a proportional-derivative controller and a linear quadratic regulator are implemented in the equations of motion. Floquet Theory is used to check the stability of the control laws, and an optimization method further optimizes the results.

Proportional-Derivative Controller (PD):

In a proportional-derivative, or P-D, Controller, the magnetic torque, $'g_m'$, is written as:

$$(2.44) \quad g_m = -(K_p \theta + K_d \dot{\theta})$$

Where $'K_p'$ and $'K_d'$ are gain matrices. The proportional gain matrix, $'K_p'$ and the derivative gain matrix, $'K_d'$ can be represented by:

$$(2.45) \quad \mathbf{K}_p = \begin{bmatrix} K_{p11} & K_{p12} & K_{p13} \\ K_{p21} & K_{p22} & K_{p23} \\ K_{p31} & K_{p32} & K_{p33} \end{bmatrix} \quad \mathbf{K}_d = \begin{bmatrix} K_{d11} & K_{d12} & K_{d13} \\ K_{d21} & K_{d22} & K_{d23} \\ K_{d31} & K_{d32} & K_{d33} \end{bmatrix}$$

For this controller, the attitude and angular velocity error are fed back into the system. The challenge of a P-D controller is determining gain matrices that damp the system.

After the 18 elements in the two gain matrices are chosen, the resulting system is examined the check for damping. The elements are altered to obtain desired results. In this application, the gain matrices are constrained to be diagonal to reduce the number of elements that can be altered from 18 to six.

Application of Floquet theory:

Floquet's¹¹ theory describes dynamic systems in which the coefficients are periodic. This theory has applications that are directly applicable to the magnetic control problem. After the controller gain is calculated for the time invariant linear equations, the stability of the gains in the linear time variant equations is examined using Floquet's theory. For stability, Q must be chosen such that the eigenvalue of or the monodromy matrix, is located inside the unit circle, where:

$$(2.46) \quad \mathcal{X}(T) = [\mathbf{x}_1(T) \quad \mathbf{x}_2(T) \quad \cdots \quad \mathbf{x}_6(T)]$$

Using initial values:

$$(2.47) \quad \mathcal{X}(0) = [\mathbf{x}_1(0) \quad \mathbf{x}_2(0) \quad \cdots \quad \mathbf{x}_6(0)] = \begin{bmatrix} 1 & 0 & \cdots & 0 \\ 0 & 1 & \cdots & 0 \\ \vdots & \vdots & \ddots & \vdots \\ 0 & 0 & \cdots & 1 \end{bmatrix}$$

With the control gain matrix known, the linear system:

$$(2.48) \quad \dot{\mathbf{x}} = \mathbf{F}\mathbf{x} - \mathbf{G}(t)\mathbf{K}\mathbf{x}$$

Is solved.

The mapped magnetic moment is then equal

$$(2.49) \quad \tilde{\mathbf{M}}(t) = -\mathbf{K}\mathbf{x}$$

and applied magnetic moment is equal to:

$$(2.50) \quad \mathbf{M}(t) = \frac{\tilde{\mathbf{M}}(t) \times \mathbf{B}(t)}{\|\mathbf{B}(t)\|}$$

This is implemented in the linear time varying system of equations for control.

Optimization of Q:

As 'Q' is varied, different values of 'K' are obtained. An optimum 'Q' exists which leads to a set of gains that damp the system in the least time. This optimum 'Q' occurs for the linear time varying case when the eigenvalues of the matrix, ' $\mathcal{X}(\mathcal{T})$ ' are closest to the origin. A Nelder-Mead Simplex¹², or direct search, method is used as the minimizer. This method has a few disadvantages because it cannot consider constraints in the system and is not the most efficient minimizer. However, the Nelder-Mead simplex method is useful in this application because it can deal with multidimensional problems and does not require derivatives, so it takes less computation time.

The eigenvalues of $'\mathcal{X}(\mathcal{T})'$ are minimized to determine the values of $'\mathbf{Q}'$ leading to the optimal gain matrix for the linear time varying system. The cost function used in the optimization is equal to the sum of the squares of the eigenvalues of $'\mathcal{X}(\mathcal{T})'$.

A secondary method of optimization can be used to optimize the results of the control laws.

This method involves examining the eigenvalues of the $'\mathcal{X}(\mathcal{T})'$ matrix. The largest eigenvalue of $'\mathcal{X}(\mathcal{T})'$ is identified and the corresponding eigenvector is isolated. The $'\mathbf{Q}'$ value corresponding to the largest value in the isolated eigenvector is altered. This method is used with trial and error to obtain favorable results. Implementation of Gains in Nonlinear System. The constant gain matrix determined from the linear quadratic regulator can be implemented in the nonlinear system.

However, since these gains were formed using the linear time invariant system and optimized for use in the linear time varying system, there is no guarantee that the nonlinear system will be stable. The results from each nonlinear simulation must be individually examined to check for stability. The linear quadratic regulator method of control is summarized in **Figure 2.8**.

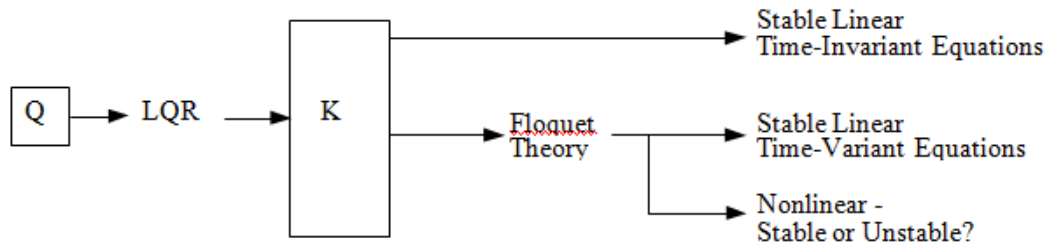


Figure 2.9: Summary of LQR Method (obtained from reference 19)

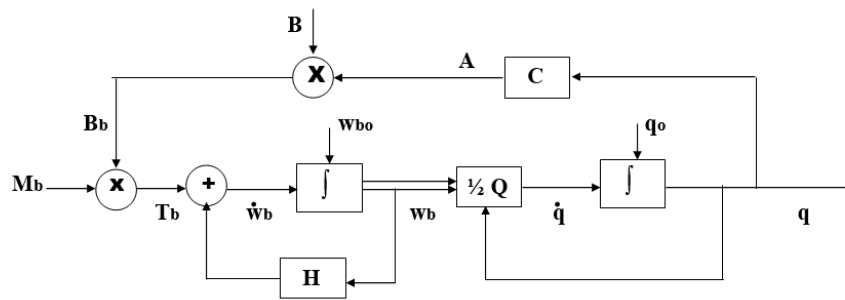
Equations (2.40) – (2.56) obtained from reference 18, 19, and 20.

CHAPTER 3 MODEL AND RESULTS

In this chapter the model of the system and animation of the satellite presented. First and second parts of the chapter will explain the design of the model, the model design on two subsystems, one is for the satellite attitude determination and control and the other one is for visual representation of this satellite in running simulation. The third part of the chapter is the results collected and discussed. Lets have a look more closely.

3.1 model

First step is to convert the designed dynamic system :



Symbols

- A** Attitude matrix , see Wertz (12-2)
- M** Dipole moment of satellite coils
- w** Angular velocity of satellite

- B** Earth's Magnetic Field
- T** Torque exerted on satellite by coils $T = M \times B$
- q** Attitude of satellite given as a quaternion

$$Q = \begin{pmatrix} 0 & w_{bz} & -w_{by} & w_{bx} \\ -w_{bz} & 0 & w_{bx} & w_{by} \\ w_{by} & -w_{bx} & 0 & w_{bz} \\ -w_{bx} & -w_{by} & -w_{bz} & 0 \end{pmatrix} \text{ see Wertz (16-2b)}$$

- H** expresses Euler equations, see Wertz (16-50)
- $\dot{w}_{bx} = k_1 w_{by} w_{bz} + T_{bx}$
- $\dot{w}_{by} = k_1 w_{bz} w_{bx} + T_{by}$
- $\dot{w}_{bz} = k_1 w_{bx} w_{by} + T_{bz}$

C converts **q** to **A** see Wertz (12-13a)

Note: 1. **b** denotes the vector components are referred to satellite Body axes.
 eg. **B** Earth's Field wrt Inertial axes. **B_b** Earth's Field wrt Body axes.
 If **V** is any vector, **V_b** = **A V** see Wertz (12-4)
 2. I use **x y z** for the body axes where Wertz uses **u v w** (12-2)

Figure 3.1 : Designed Dynamics system of amature satellite (drawn by Jonathan Henderson, KiwiSat team member)

The model was created in software specially designed for mathematical computations and

simulations called Matlab.

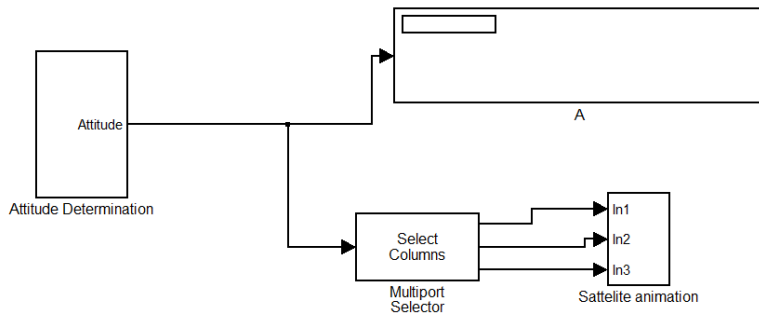


Figure 3.2: The simulation model

Those two blocks represent simulation of the satellite dynamics and the animation created for visual representation.

The first block looks like this Inside:

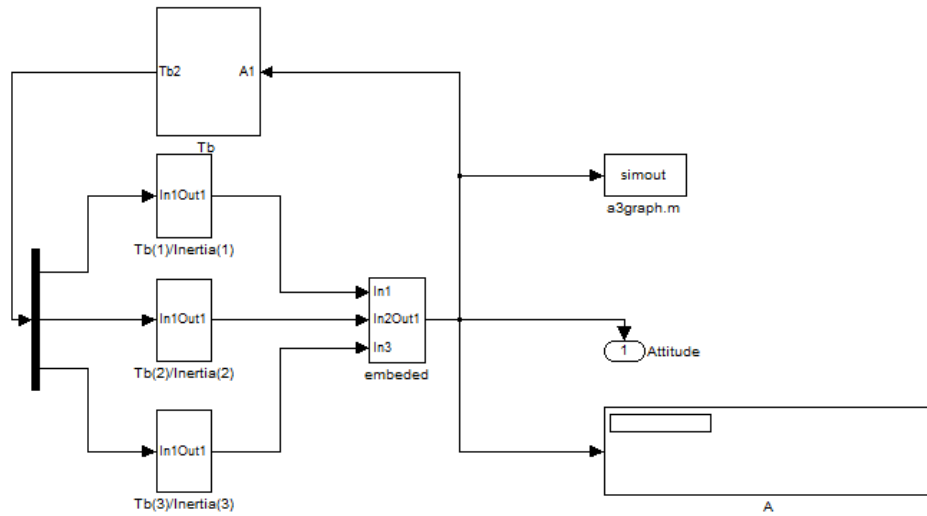


Figure 3.3: attitude determination and control box

And if we open our embedded system block, we have a system looks like this:

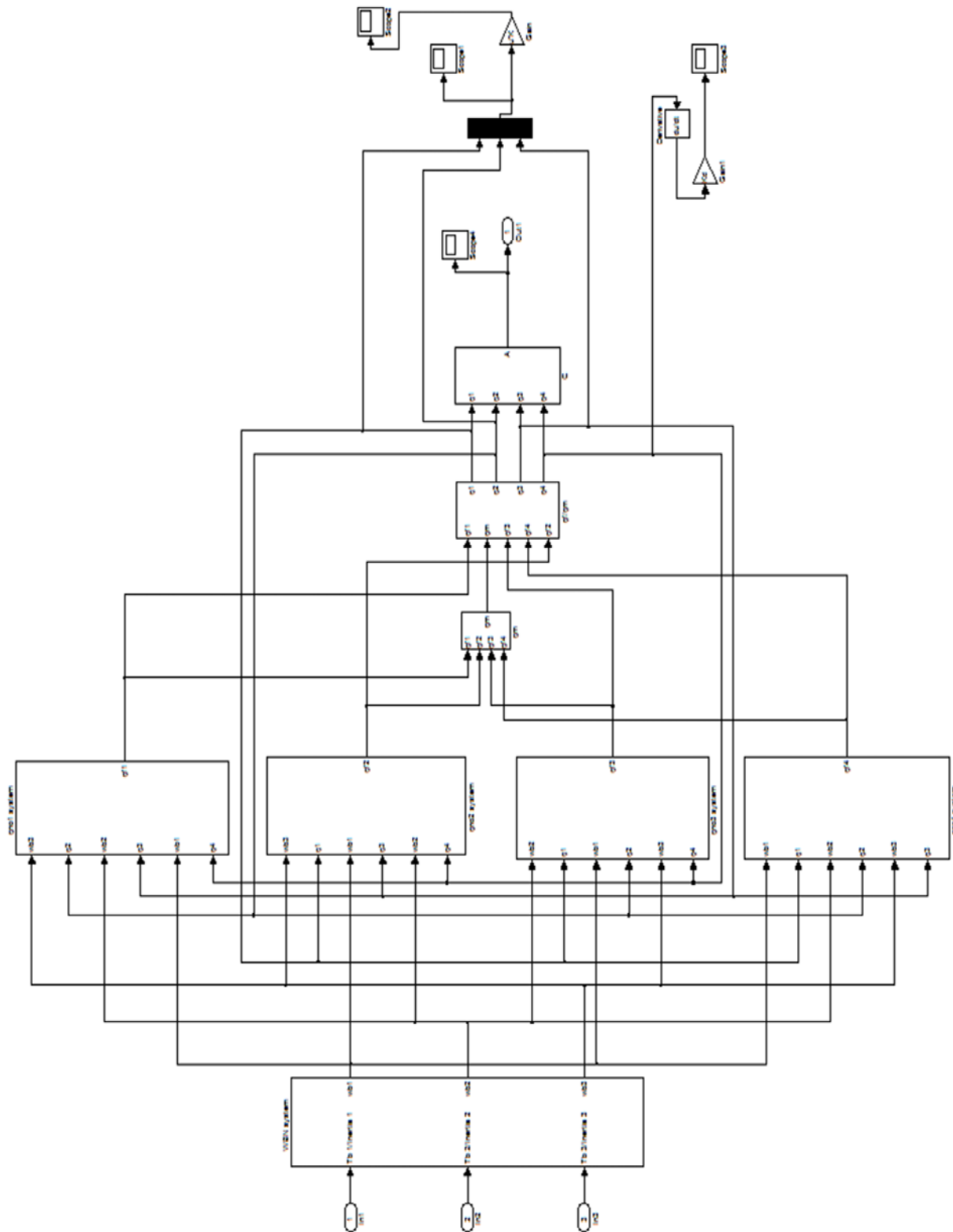


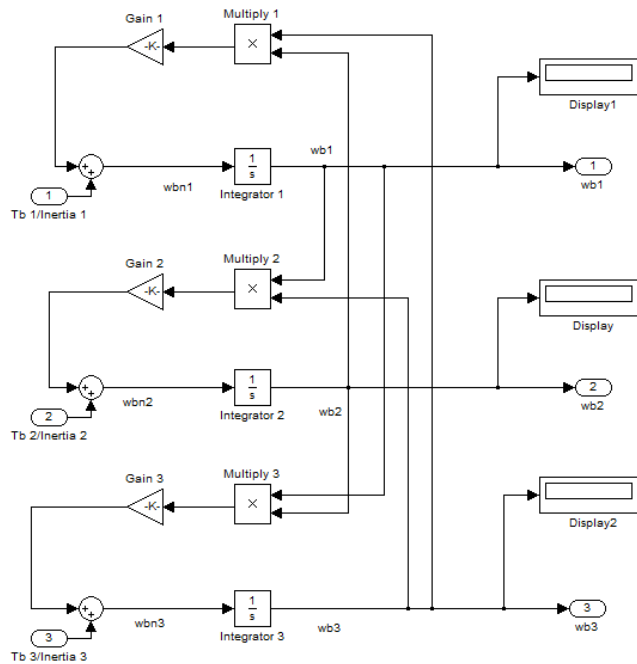
Figure 3.4: Embedded block diagram

Let's have a look more closely into this block:



This block represents the angular velocity of the satellite, we can see that torque from magnetic coils is one of the main components for this block of the system, and it's logical as the angular velocity changes with amount of torque applied.

Inside of this block:



And the output of this system presented as the graph:

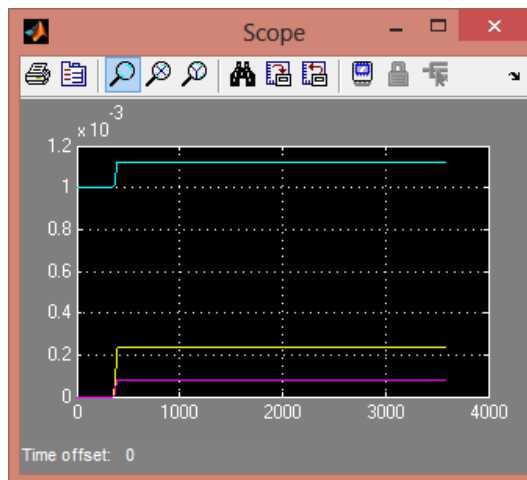
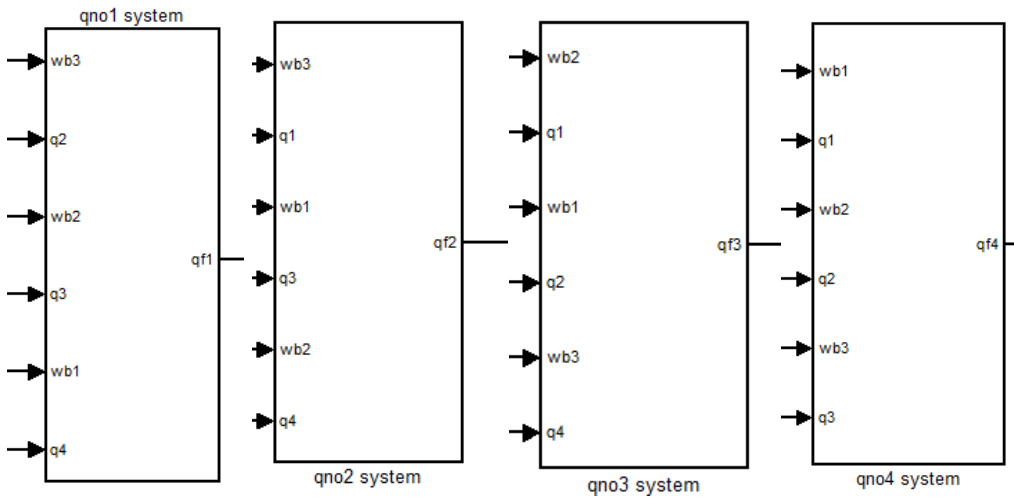


Figure 3.5: Angular velocity stabilization

Next four blocks represent our quaternions:



To find out more about quaternions please refer to chapter 2.1.2 equation (2.42)

The Graph 2 represent the rotation of the satellite each line represent the value of quaternion (q1, q2, q3, q4):

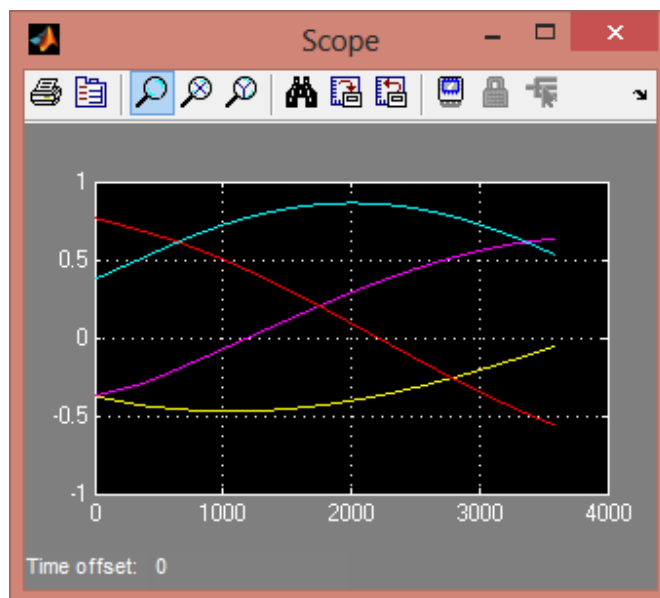
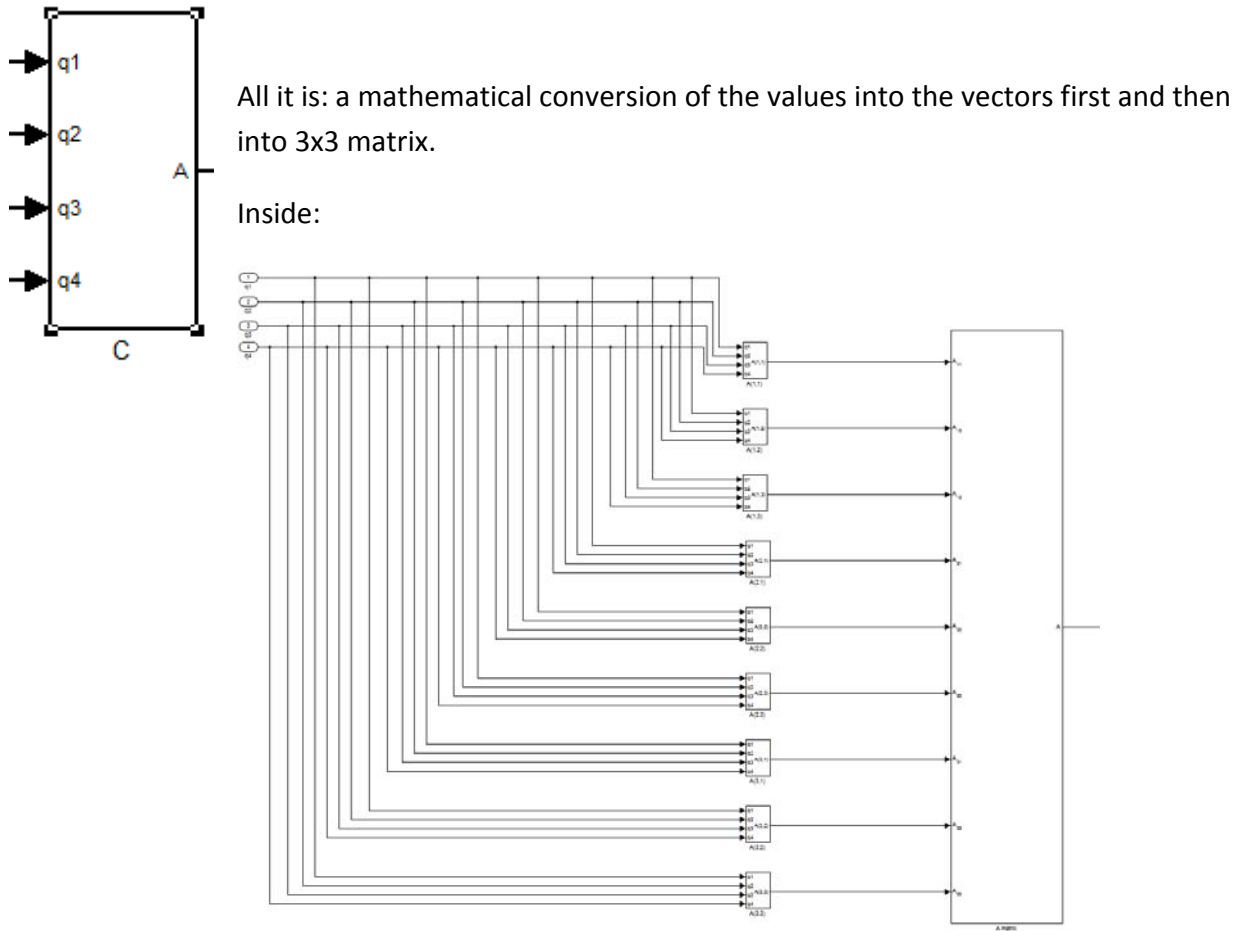


Figure 3.6: behavior of satellite.

From this graph we can see that the satellite is turning.

One of the most important blocks is a block named “C” which is converts quaternion values into attitude matrix “A”:



The graph 3.3 represent the Attitude matrix “A” needed for simulation

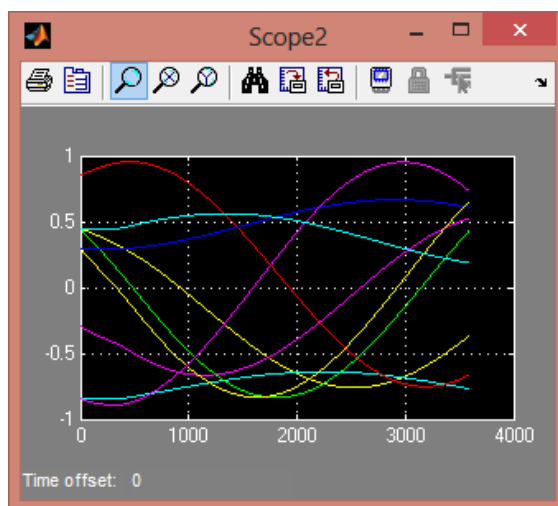
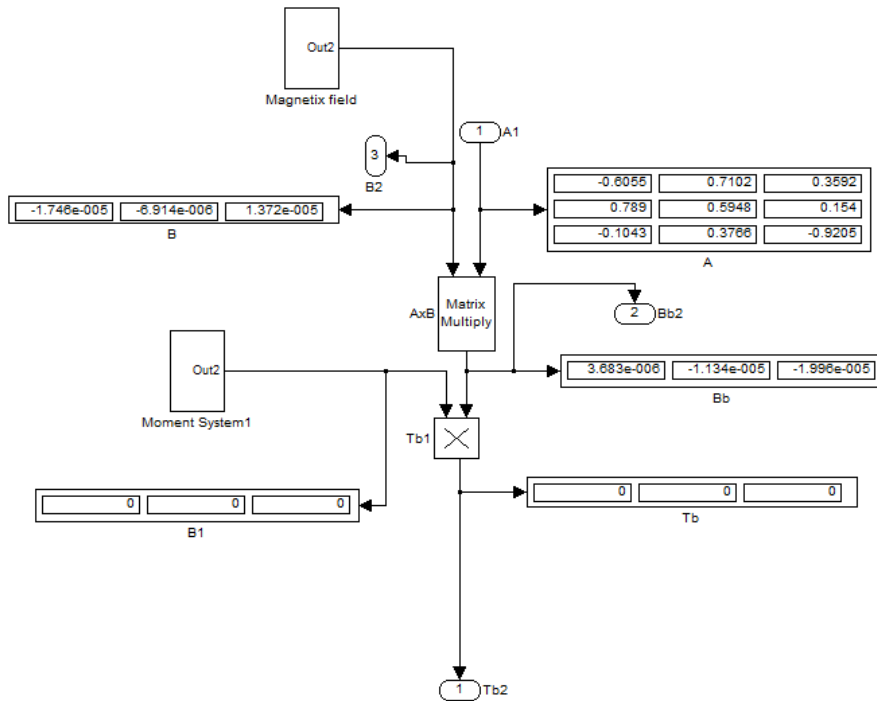


Figure 3.7: Attitude Matrix

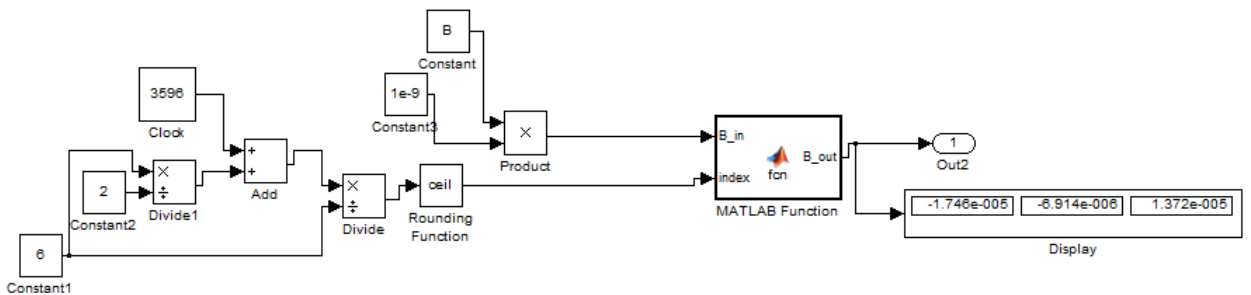
The other two blocks normalization of the quaternions and finding the average.

That concludes our embedded part of the model.

Another block I would like to talk about is the calculation and simulation of torque:



The main difficulty was to do a cross credit of two matrixes: multiply of attitude “A” and magnetic field “B” with moment matrix “Mb”, the special C++ functions were created to make sure the calculation is correct for the “B”:

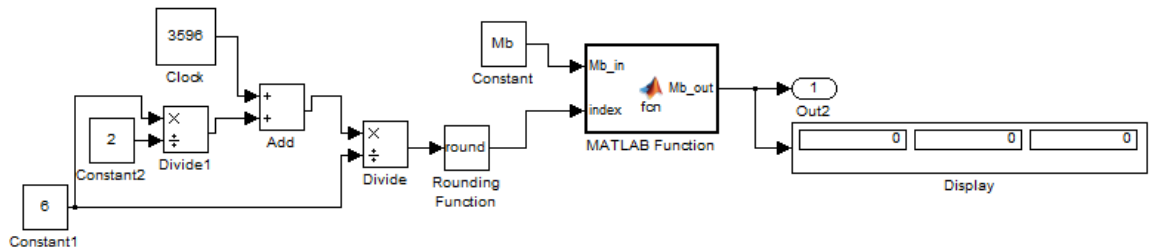


The function is called B_out:

```
function B_out = fcn(B_in,index
```

$B_out = B_in(index,:);$

And for “Mb”:

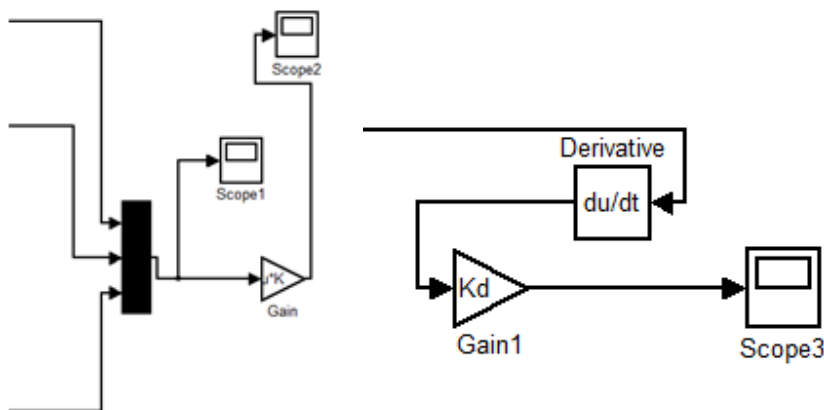


The function called Mb_out:

```
function Mb_out = fcn(Mb_in,index)
```

```
Mb_out = Mb_in(index,:);
```

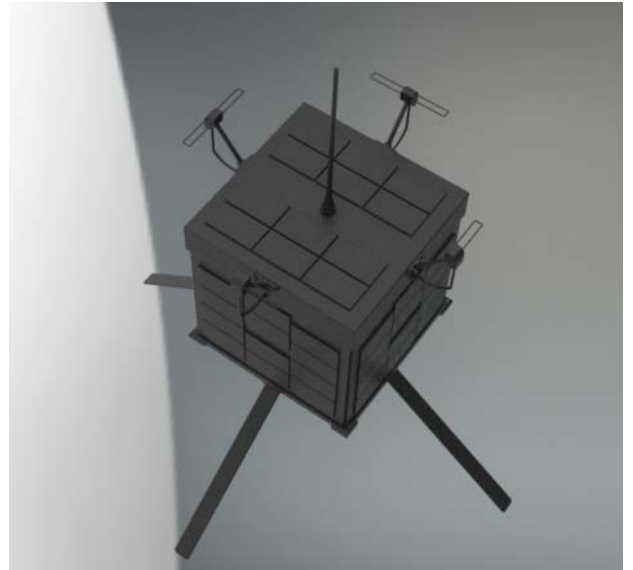
Next part of the model is a control blocks:



Those blocks represent the P-D controller method applied to the system, different values applied for the Gain K_d , K_p more about them in the results section of this chapter.

3.2 Animation

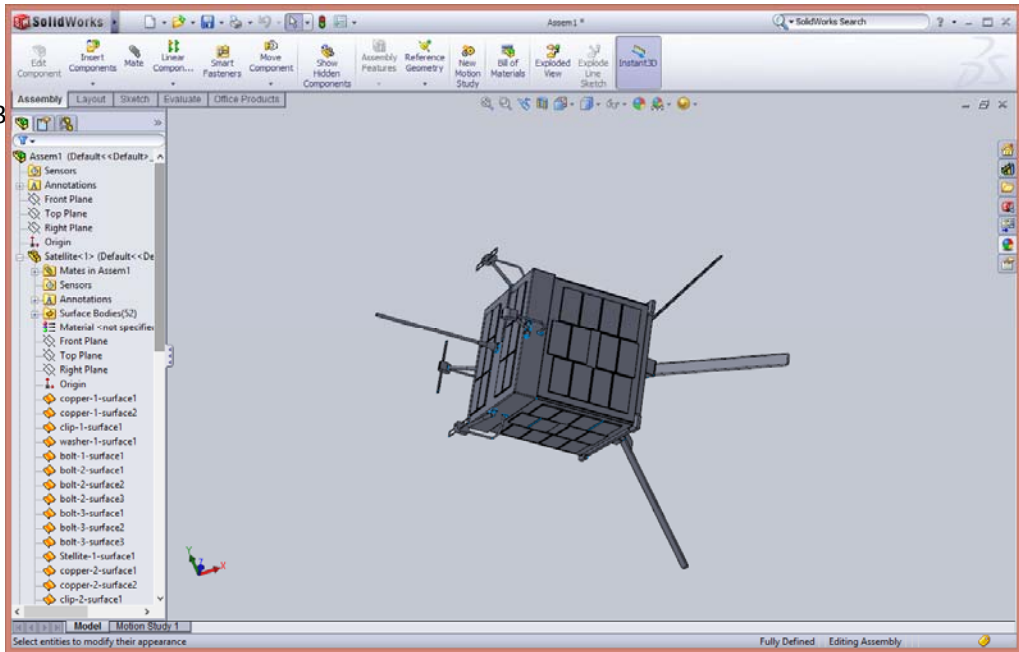
This part of the chapter explains how the satellite model was designed and converted into simulation.



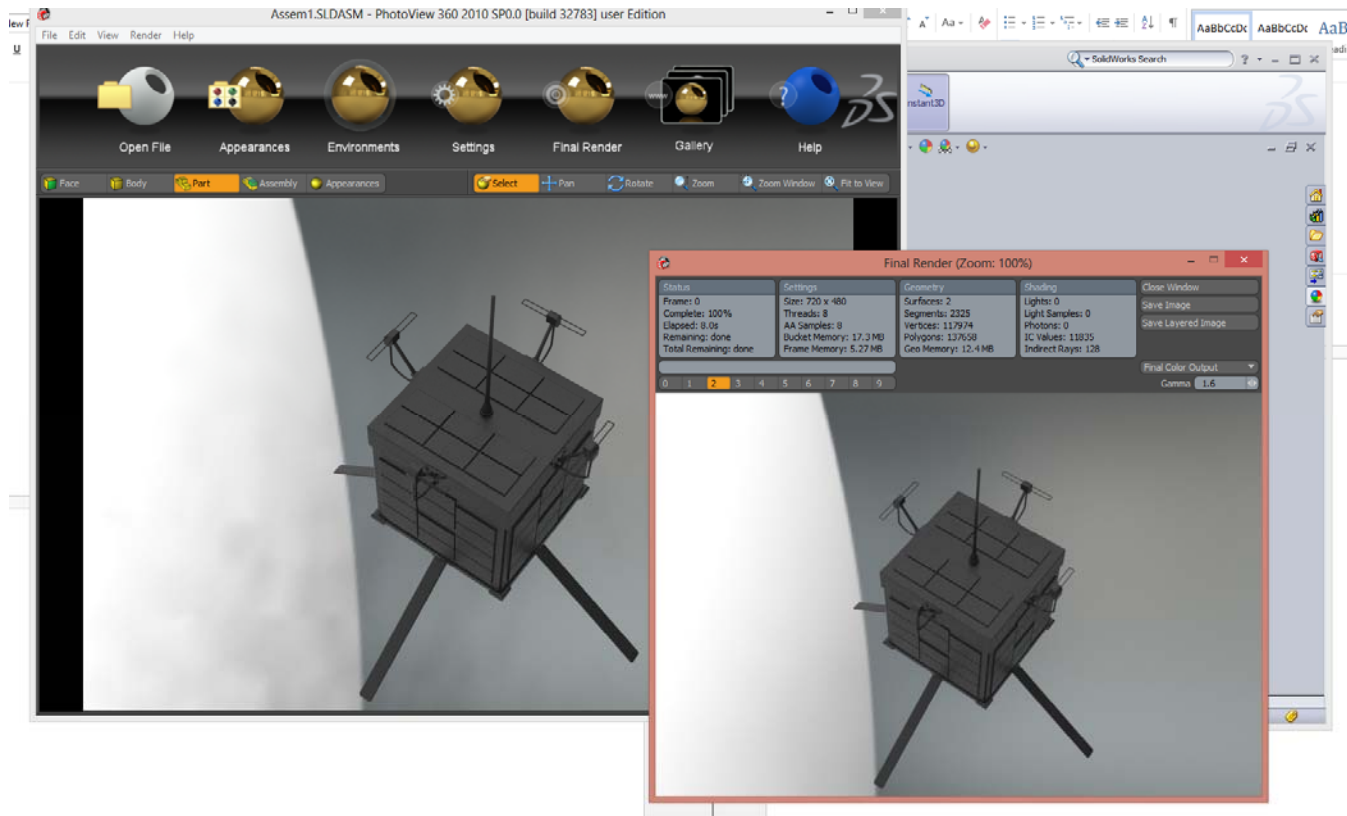
Final design:

Figure 3.8: 3D model of the satellite.

The above model was created in Solidworks Software:



Then rendered in the photo 360 software:

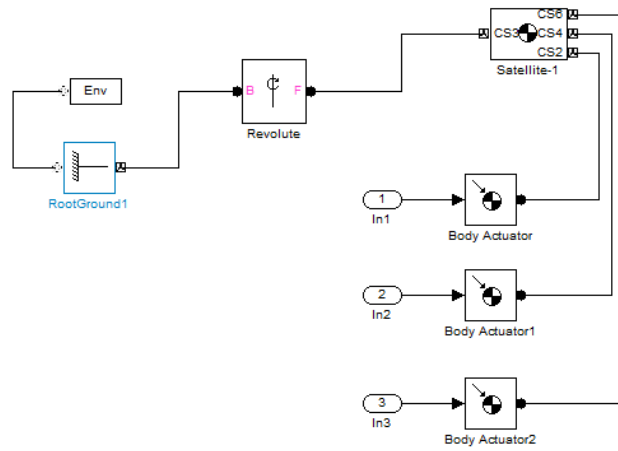


And finally converted to Matlab SimMechanics using software “SimMechanics Link”: using those steps:

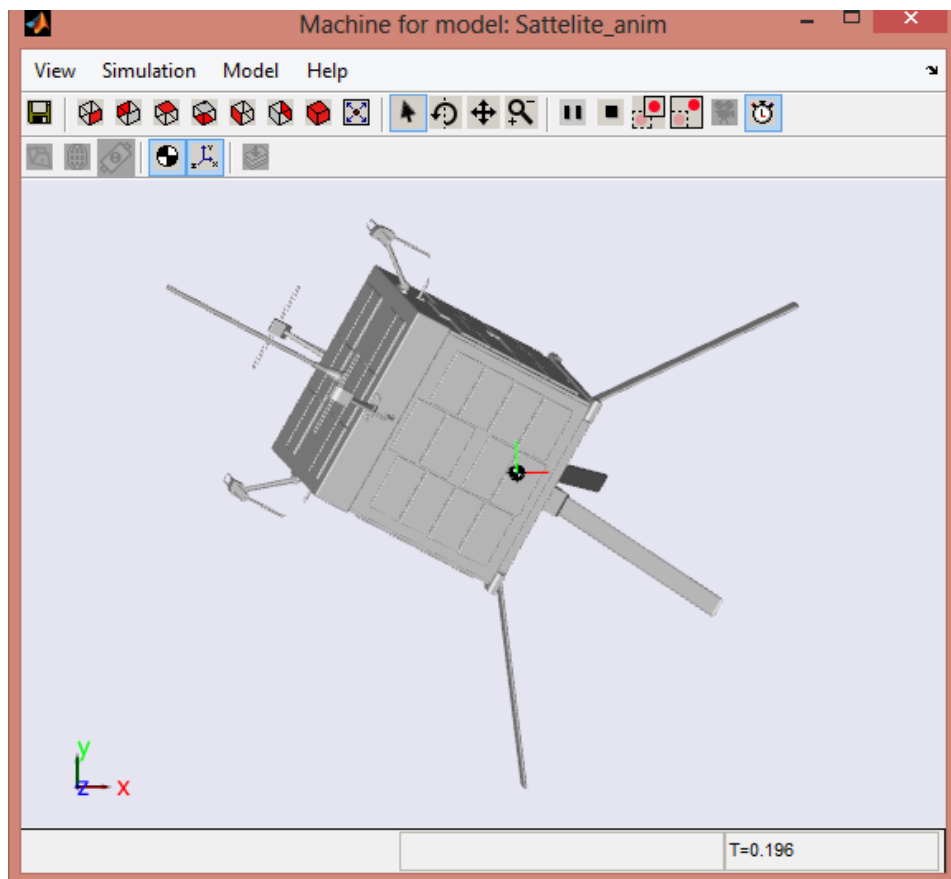
- 1) Start MATLAB and install the SimMechanics Link add-on by entering the following MATLAB command: `install_addon('<file of the SimMechanics folder >')`
- 2) From the MATLAB command line, enter `smlink_linksw`. You see a message indicating a successful link.
- 3) `import_physmod('<Assem1>.xml')` (solidworks .xml file)

That converts the 3D model into model created by mathematical functions, with parameters such as torque, inertia and axis.

The below model is the SimMechanics representation of the satellite body.



And the simulation looks like this:



3.3 Results

The control laws for magnetic control are tested in this chapter through computer simulations. Simulations are performed using Matlab and examine the stability of the system for both linear and nonlinear equations using a proportional-derivative controller and a constant coefficient linear quadratic regulator. By altering the input values, different cases can be simulated. The outputs are plotted and compared.

Inputs

The inputs to the simulation include the geometry of the spacecraft, its initial orbit and attitude, and the gain characteristics. The initial orbital position is:

- $a = 6764.44 \text{ km}$
- $e = 0.0083636$
- $i = 98.1662^\circ$
- $\Omega = 356.9^\circ$
- $\omega = 196.8473^\circ$
- $v = 282.4533$

The Initial Attitude characteristics :

The initial attitude characteristics are:

$$\bar{q}^{bo} = \begin{bmatrix} 0.04963 \\ 0.11436 \\ 0.00138 \\ 0.99220 \end{bmatrix} \quad w^{bo} = \begin{bmatrix} 3.1540 \times 10^{-3} \\ 6.9167 \times 10^{-3} \\ 1.2041 \times 10^{-3} \end{bmatrix}$$

which is approximately 14 degrees out of plane from the desired nadir pointing orientation.

The moment of Inertia matrix, I :

$$I = \begin{bmatrix} 1 & 0 & 0 \\ 0 & 1.4 & 0 \\ 0 & 0 & 0.6 \end{bmatrix}$$

The gain inputs are in the form of \mathbf{Kp} and \mathbf{Kd} , which are 3×3 matrices, when the PD controller is used, and \mathbf{Q} , which is a 6×6 diagonal matrix, for the linear quadratic regulator technique.

Outputs

The Matlab simulation determines the time varying spacecraft attitude and angular velocity in the form $\overline{q_{bo}}$ and w_b^{bo} . In addition, the simulation outputs the time varying magnetic moment. This value represents the amounts of moment the magnetic torque system is required to produce.

No Magnetic Control

Lack of magnetic control was simulated by setting the gains, \mathbf{K} , equal to zero. A simulation was performed for the linear system with Euler angles, the linear system with quaternions, and the nonlinear system

For initial 14 degrees system:

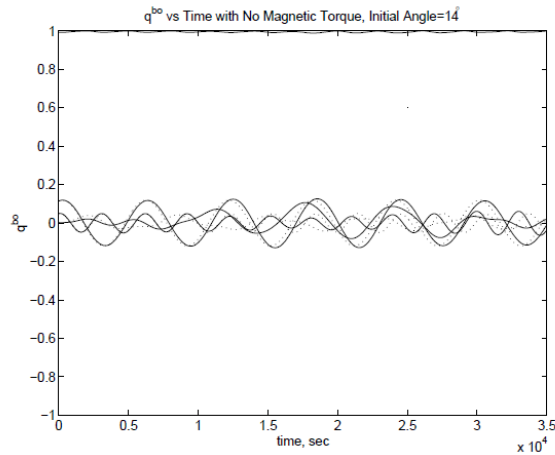


Figure 3.9: Quaternions with No Magnetic Torque, Initial Angle=14

The simulation was also performed with the initial conditions closer to the desired position:

$$\bar{q}^{bo} = \begin{bmatrix} 0.01990 \\ 0.04584 \\ 0.00550 \\ 0.99875 \end{bmatrix} \quad w^{bo} = \begin{bmatrix} 3.306 \times 10^{-3} \\ 6.851 \times 10^{-3} \\ 1.171 \times 10^{-3} \end{bmatrix}$$

Which corresponds to an initial rotation of approximately 6 degrees from desired:

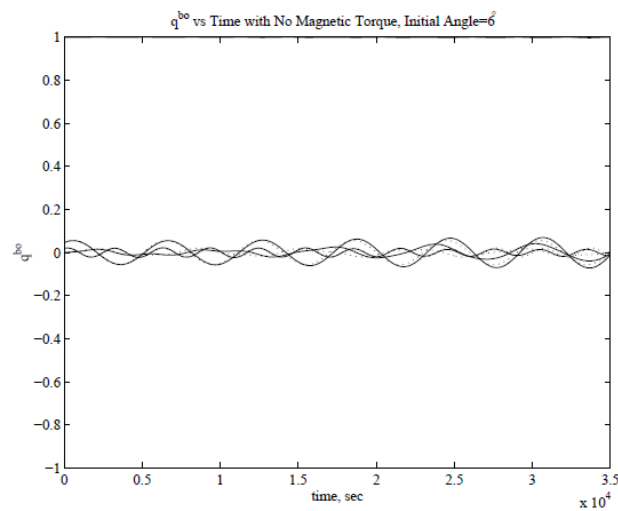


Figure 3.10: Quaternions with No Magnetic Torque, Initial Angle=6

From the graphs we can see if we closer to desired rotation the error is less.

Magnetic Control

The magnetic controller is implemented. The time it takes to stabilize the satellite is examined, as well as the magnetic moment required for its maneuver.

The following gains are implemented in the linear equations:

$$K_d = \begin{bmatrix} 0.005 & 0 & 0 \\ 0 & 0.005 & 0 \\ 0 & 0 & 0.005 \end{bmatrix} \quad K_p = \begin{bmatrix} 0.0001 & 0 & 0 \\ 0 & 0.0001 & 0 \\ 0 & 0 & 0.0001 \end{bmatrix}$$

As the magnitude of the proportional derivative, K_p is decreased, the frequency of oscillations decreases. If the derivative gain, K_d is increased, the system damps faster.

The quaternion for the system using the above gains is shown in Graph 3.6 in a close-up view.

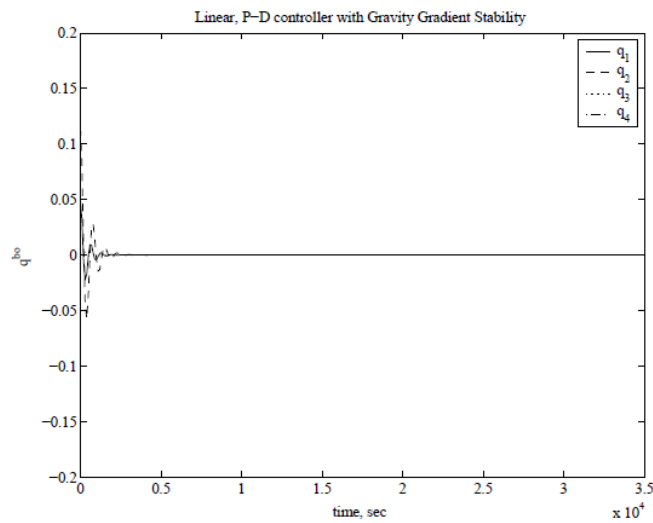


Figure 3.11: Quaternion for P-D Controller with assigned gains.

Constant Coefficient Linear Quadratic Regulator

For the constant coefficient linear quadratic regulator, the value of the weight matrix, \mathbf{Q} :

$$\mathbf{Q} = \begin{bmatrix} 0.001 & 0 & 0 & 0 & 0 & 0 \\ 0 & 0.001 & 0 & 0 & 0 & 0 \\ 0 & 0 & 0.001 & 0 & 0 & 0 \\ 0 & 0 & 0 & 0.001 & 0 & 0 \\ 0 & 0 & 0 & 0 & 0.001 & 0 \\ 0 & 0 & 0 & 0 & 0 & 0.001 \end{bmatrix}$$

This leads to a gain matrix, \mathbf{K} , of:

$$K = \begin{bmatrix} 0.0014 & 0 & -0.0038 & 16.1206 & -0.1190 & -1.1532 \\ -0.0001 & 0.0051 & 0 & -0.0688 & 29.7242 & -0.0501 \\ 0.0121 & 0 & 0.0056 & -0.7335 & 0.0334 & 32.8568 \end{bmatrix}$$

With these gains, the eigenvalues of the matrix are located inside the unit circle, as shown in Graph 3.7.

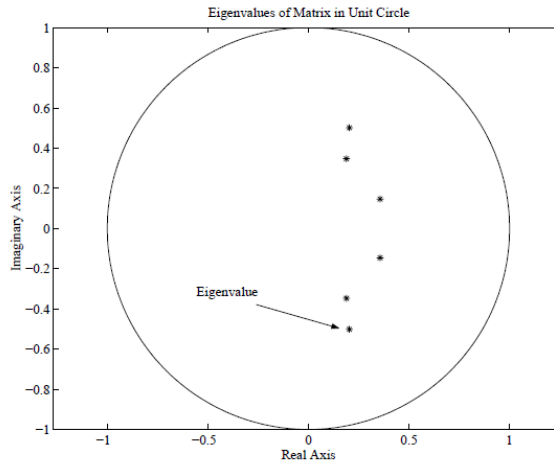


Figure 3.12: Eigenvalues of X(t)

Since the eigenvalues are all inside of the unit circle, the linear equations are stable over time:

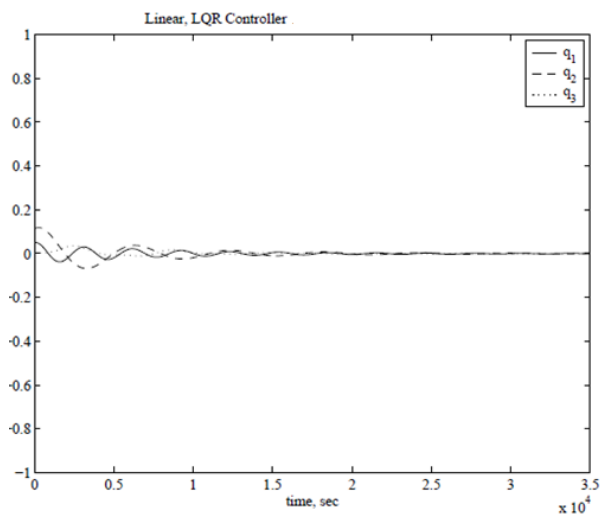


Figure 3.13: Quaternion for Linear, LQR Controller

The magnetic moment required experiences long period oscillations over time. These oscillations are evident when the magnetic moment is plotted over a long period of time in Graph 3.9. In this case, one period is equal to approximately six days, and this periodic nature occurs because of the relative rotation between the Earth and the magnetic field, coupled with the orbital position. These long period oscillations exist in all of the cases examined.

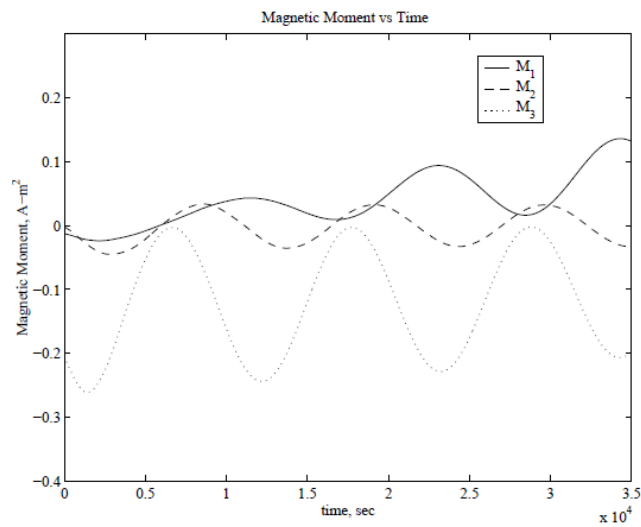


Figure 3.14: Magnetic Moment

Chapter 4

Discussion and conclusion

4.1 Discussion

The attitude determination and control system for KiwiSat amateur satellite is designed and tested. The attitude determination model was created and tested in Simulink program that is part of the Matlab (mathematical software) package, the magnetic control was taken into account, as the magnetic field of the earth was designed for the simulation using above mentioned software.

Control method was chosen and carried over, which proved to be efficient in the long run (stabilization of 6 days), not so effective when the position of the satellite need to be aligned fast.

Simulation was performed with various configurations and conditions. The gain for the controller was varied to find the desired equilibrium. It was determined that the satellite can be stabilized with magnetic control, by applying magnetic moments with magnitudes suitable for this size of satellite.

In the design of P-D controller, which have two gain matrices K_p , K_d with total of 18 elements that can be changed to check for further stability.

4.2 Conclusion

As stated above the desired outcome was achieved by design system, however further research needed for finding more efficient method of control, to be able to stabilize the position fast and to carry over tasks with precision.

Reference

- 1) Carl R. Nave. HyperPhysics. Georgia State University, 2000.
- 2) Steven A. Macintyre. The Measurement, Instrumentation and Sensors Handbook, chapter Magnetic Field Measurement. CRC Press LLC, 1999.
- 3) Magnetic Fields - Earth and Extraterrestrial. Technical Report NASA SP-8017, National Aeronautics and Space Administration, March 1969.
- 4) Geological Survey of Canada. <http://www.geolab.nrcan.gc.ca/geomag>.
- 5) Ye Shi-hui. Magnetic Fields of Celestial Bodies. Kluwer Academic Publishers, Dordrecht, 1994.
- 6) United States Geological Survey. Geomagnetism. <http://geomag.usgs.gov>
- 7) Wallace H. Campbell. Introduction to Geomagnetic Fields. Cambridge University Press, Cambridge, 1997.
- 8) Francis W. Sears, Mark W. Zemansky, and Hugh D. Young. University Physics. Seventh edition, 1995.
- 9) John A. Sorenson. A Magnetic Attitude Control System for an Axisymmetric Spinning Spacecraft. Journal of Spacecraft and Rockets, May 1971.
- 10) Anon. Spacecraft Magnetic Torques. Technical Report NASA SP-8018, National Aeronautics and Space Administration, March 1969
- 11) Carlo Arduini and Paolo Baiocco. Active Magnetic Damping Attitude Control for Gravity Gradient Stabilized Spacecraft. Journal of Guidance Control and Dynamics, January-February 1997.
- 12) Marcel J. Sidi. Spacecraft Dynamics and Control, A Practical Engineering Approach. Cambridge Aerospace Series. Cambridge University Press, Cambridge, 1997
- 13) Dominic M. Florin. Three Axis Spacecraft Attitude Control and Dynamics with Permanent Magnets. Master's thesis, Utah State University, 2001.
- 14) Roger R. Bate, Donald D. Mueller, and Jerry E. White. Fundamentals of Astrodynamics. Dover Publications, Inc, New York, 1971
- 15) U.S. Naval Observatory. Web MICA (Multiyear Interactive Computer Almanac). <http://aa.usno.navy.mil>
- 16) Christopher Hall. Attitude Determination and Control Course Notes. Virginia Tech

- 17) James R. Wertz and Wiley J. Larson, editors. Space Mission Analysis and Design. Microcosm Press, El Segundo, California, third edition, 1999.
- 18) Rafal Wirsniewski. Satellite Attitude Control Using Only Electromagnetic Actuation. PhD thesis Aalborg University, Dec 1996
- 19) Rafal Wirsniewski. Linear Time Varying Approach to Satellite Attitude Control Using Only Electromagnetic Actuation. AIAA Guidance Navigation and Control Conference. New Orleans, LA, August 11-13 1997
- 20) Keith L. Musser and Ward L. Ebert. Autonomous Spacecraft Attitude Control Using Magnetic Torqueing Only. Flight Mechanics/Estimation Theory Symposium. May 23-24 1989. NASA Conference Publication.
- 21) Ronald T. Merrill and Michael W. McElhinny. Earth's Magnetic Field, 1983
- 22) National Geophysical Data Center. The Geomagnetic field
- 23) James R. Wertz. Spacecraft Attitude Determination and control. 2000
- 24) J.S. White, F.H. Shigemot, and K. Bourquin. Satellite Attitude Control Utilizing the Earth's Magnetic Field. Technical Report, 1961
- 25) Felix R. Hoots and Ronald L. Roehrich. Models for propagation of NORAD Element Sets, 1988
- 26) Fred Kennedy. Kiwisat Science package proposals, 2011

Appendix

Separate matlab file created to calculate the IGRF 10 model that creates simulation of earth magnetic field:

```
function field=IGRF10(altitude,latitude,longitude)
% Function to compute X, Y, Z components of Earth's Magnetic Field
% (nT) at single point close to the surface of the earth.
% Note at Auckland, latitude = -36.6, longitude = 175

longrad = pi*(longitude+180)/180;
% Note 180deg ADDED,
% because in math model, zero of longitude occurs at int date line.
latradg = pi*latitude/180;

A = 6378.137;
B = 6356.7523;
k0 = altitude;
k1 = sqrt((A*cos(latradg))^2+(B*sin(latradg))^2);
k2 = (A*A*cos(latradg))^2+(B*B*sin(latradg))^2;
latrad = atan(tan(latradg)*(k0*k1+B*B)/(k0*k1+A*A));
r = sqrt(k0^2 + 2*k0*k1 + k2/(k1*k1));
psi = latrad - latradg;

% World Magnetic Model coefficients
t = 2.5; % Decimal time in yr from Yr 2005
wmm_coef = [-295568 0 80 0; -16717 50798 106 -209; -23406 0 -151 0;
30469 -25947 -78 -232; 16570 -5167 -8 -146; 13354 0 4 0;
-23051 -1999 -26 50; 12467 2693 -12 -70; 6740 -5242 -65 -6;
9198 0 -25 0; 7981 2815 28 22; 2113 -2260 -70 16; -3794 1458 62 58;
1000 -3047 -38 1; -2274 0 -28 0; 3546 424 7 0; 2087 1798 -32 17;
-1365 -1230 -11 21; -1683 -195 1 48; -141 1036 -8 -11; 732 0 -7 0;
697 -203 4 -6; 767 547 -3 -19; -1512 636 23 -4; -149 -634 -21 -5;
146 -1 -6 -3; -863 504 14 7; 801 0 2 0; -745 -615 -1 6; -14 -224 -3 4;
385 72 11 2; 124 254 6 3; 95 110 5 -8; 57 -264 -4 -2; 18 -51 6 1;
249 0 1 0; 77 112 3 -2; -116 -210 -4 1; -69 96 3 3; -182 -198 -3 4
100 161 2 1; 92 77 4 -2; -116 -129 -7 4; -52 -2 4 4; 56 0 0 0;
99 -201 0 0; 35 129 0 0; -70 126 0 0; 51 -67 0 0; -108 -81 0 0
-13 8 0 0; 88 29 0 0; -67 -79 0 0; -91 60 0 0; -23 0 0 0; -63 24 0 0;
```

```

16 2 0 0; -26 44 0 0; 0 48 0 0; 31 -65 0 0; 4 -11 0 0; 21 -34 0 0;
39 -8 0 0; -1 -23 0 0; -23 -79 0 0; 28 0 0 0; -16 3 0 0; -17 12 0 0;
17 -8 0 0; -1 -25 0 0; 1 9 0 0; -7 -6 0 0; 7 -27 0 0; 18 -9 0 0;
0 -13 0 0; 11 -20 0 0; 41 -12 0 0; -24 0 0 0; -4 -4 0 0; 2 3 0 0;
8 24 0 0; -3 -26 0 0; 11 6 0 0; -5 3 0 0; 4 0 0 0; -3 0 0 0; -3 3 0 0;
-1 -9 0 0; -3 -4 0 0; -1 8 0 0];
wmm_coef = 0.1*wmm_coef;

latinc = pi/360; % Increment used for calculating gradient
a = 6371.2; % Standard Earth Reference radius in km

% Find X, Y, Z components
Xt=0;
Yt=0;
Zt=0;
for n=1:12
    SP=legendre(n,sin(latrad),'sch');
    SPgradu=legendre(n,sin(latrad+latinc),'sch');
    SPgradl=legendre(n,sin(latrad-latinc),'sch');
    nn = n*(n+1)/2;
    Xm=0;
    Ym=0;
    Zm=0;
    for m=0:n
        gcos = (wmm_coef(nn+m,1) + t*wmm_coef(nn+m,3))*cos(m*longrad);
        hsin = (wmm_coef(nn+m,2) + t*wmm_coef(nn+m,4))*sin(m*longrad);
        gsin = (wmm_coef(nn+m,1) + t*wmm_coef(nn+m,3))*sin(m*longrad);
        hcos = (wmm_coef(nn+m,2) + t*wmm_coef(nn+m,4))*cos(m*longrad);
        Xm = Xm + (gcos+hsin)*((-1)^m)*SPgradu(m+1)-((-1)^m)*SPgradl(m+1))/(2*latinc);
        Ym = Ym + m*(gsin-hcos)*((-1)^m)*SP(m+1);
        Zm = Zm + (gcos+hsin)*((-1)^m)*SP(m+1);
    end
    Xt=Xt+Xm*(a/r)^(n+2);
    Yt=Yt+Ym*(a/r)^(n+2);
    Zt=Zt+Zm*(n+1)*(a/r)^(n+2);
end
X = -(Xt*cos(psi) - Zt*sin(psi)); % northward
Y = Yt/cos(latrad); % eastward
Z = -(Xt*sin(psi) + Zt*cos(psi)); % downward
field=[X, Y, Z];

```

And another program to calculate Orbit:

```

function [rad,lat,lon,lonc] = Orb_AO51(t1)
% Function to give radial dist, lat, long, of satellite

```

```

% starting from (decimal) day of year (day)
% at 600 data points in intervals of 10 sec.
% Based on SGP - retaining only secular perturbations

% Orbit parameters (KEPs) at epoch
to = 143.69622809; % Time of epoch (23/May/06)
eo = 0.0083636; % Eccentricity of orbit
io = 98.1662; % Inclination of orbit (deg)
mo = 76.7305; % Mean Anomaly (deg)
no = 14.40518960; % Mean motion (rev/day)
dn = 0.00000036; % Rate of change of Mean motion (rev/day/day)
wo = 282.4533; % ARGP (deg)
Wo = 196.8473; % RAAN (deg)

ne = 360*(366.25/365.25); % Siderial Rotation of earth (deg/day)
% Find celestial longitude of Greenwich at time of epoch
ts = to - 79.7631944; % ts = Time of KEPs after vernal equinox
%pos_sun = Orb_sun(ts);
%lon_grn = pos_sun(3)-(0.5-(to-fix(to)))*360+0.8; % NOTE +0.8

a1 = (8681660.4/no)^(2/3); % Approx major semi-axis (km)
ior = (pi/180)*io;
d1 = 0.75*0.00108263*((6378.14/a1)^2)*(3*cos(ior)*cos(ior)-1)/((1-eo*eo)^(3/2));
ao = a1*(1-d1/3-d1*d1-134*d1*d1*d1/81); % Major semi-axis at epoch
% J2 Rate of change of RAAN (deg/day)
dW_dt = -1.5*0.00108263*((6378.14/ao)^2)*360*no*cos(ior)/((1-eo*eo)^2)
% J2 Rate of change of ARGP (deg/day)
dw_dt = 0.75*0.00108263*((6378.14/ao)^2)*360*no*(5*cos(ior)*cos(ior)-1)/((1-eo*eo)^2)

%nn = 600; % No of data points
%rad = zeros(nn,1);
%lat = zeros(nn,1);
%lon = zeros(nn,1);
%lonc = zeros(nn,1);

%for n = 1:nn
% t = (t1-to) + (n-1)/(24*60*6); % Time from start of orbit at 10s intervals
% Update orbit parameters
%a = ao*(no/(no+2*dn*t))^(2/3); % Major sem-axis
%Wso = Wo + dW_dt*t; % RAAN
% wso = wo + dw_dt*t; % Arg perigee
%ms = mo + 360*(no*t + dn*(t^2)); % Mean anomaly

%Wsor = (pi/180)*Wso; % Convert angles to radians
%wsor = (pi/180)*wso;
%msr = (pi/180)*ms;

```

```

% Solve Keplers equn
%mser_i = msr;          % Eccentric anomaly (initial)
%mser = mser_i+1;
%while abs(mser-mser_i) > 0.00001;
%  mser_i = mser;
%  dmser_i = (msr-mser_i+eo*sin(mser_i))/(1-eo*cos(mser_i));
%  mser = mser_i + dmser_i;
% end

% r = a*(1-eo*cos(mser));          % Radial distance
%vs = (a/r)*(1-eo*eo)*sin(mser); % Sine of true anomaly
% vc = (a/r)*(cos(mser)-eo);      % Cosine of true anomaly
% vec_o = [vc vs 0]';            % Unit dirn vector, in orbit coord

% Calculate orbit > earth coordinates. Rotation of axes matrix
%H = [cos(wsor)*cos(Wsor)-cos(ior)*sin(Wsor)*sin(wsor) -sin(wsor)*cos(Wsor)-
cos(ior)*sin(Wsor)*cos(wsor) ...
% sin(ior)*sin(Wsor); cos(wsor)*sin(Wsor)+cos(ior)*cos(Wsor)*sin(wsor) ...
% -sin(wsor)*sin(Wsor)+cos(ior)*cos(Wsor)*cos(wsor) -sin(ior)*cos(Wsor); ...
% sin(ior)*sin(wsor) sin(ior)*cos(wsor) cos(ior)];

%vec_c = H*vec_o;                % Dirn vector in earth centred inertial coord
%rad(n) = r;                      % Dist from centre of earth
%lat(n) = (180/pi)*asin(vec_c(3)); % Latitude of satellite (Cel lat = Ter lat)
%mag = sqrt(vec_c(1)*vec_c(1)+vec_c(2)*vec_c(2));
%lon_c = (180/pi)*acos(vec_c(1)/mag); % Celestial longitude of satellite
%if vec_c(2) < 0 lon_c = -lon_c;
% else end
%lonc(n)=lon_c;
% Transform from Celestial longitude to terrestrial longitude by -
% subtracting longitude of Greenwich and angle of earth's rotation since epoch.
%long = lon_c - lon_grn - ne*t;
% long = long - 360*fix(long/360); % Bring into 360 deg range
% if long < -180 long = long + 360; % Bring into -180 > +180 range
% elseif long > 180 long = long - 360;
% else end
% lon(n) = long;                  % Earth longitude of satellite
%end

```

Those two programmes are necessary for our simulation to work correctly.

After running those programs we run our simulation program:

```

%-----%
% load files %
%-----%
clear all;
load B.mat;
load Mb.mat;
tlim=3596;

%-----%
%LQ initialisation%
%-----%

Inertia = [0.115 0.115 0.115]'; % Pr Mmts of Inertia of satellite around CG. [0.2 0.2 0.05]
k = zeros(3,1); % Normalised inertia coefficients
k(1) = (Inertia(2)-Inertia(3))/Inertia(1);
k(2) = (Inertia(3)-Inertia(1))/Inertia(2);
k(3) = (Inertia(1)-Inertia(2))/Inertia(3);
%wbo =[0 0 0.001]';
%qo = [-0.3711, -0.3711, 0.3711, 0.7660]';
wbo=[0.0031540,0.0069167,0.0012041]';
qo=[0.04963,0.11436,0.00138,0.99220]';
%controler gains
Kp = [0 1 0; 0 0 1; 0 0 0];
Kd = [0 0 1; 0 0 0; 0 0 0];

Bx_o = B(1);
By_o = B(2);
Bz_o = B(3);

open('rotdyn3A.mdl');
sim('rotdyn3A');

%-----%
%coil parameters %
%-----%

%Numberof coil Windings
N_x = 110;
N_y = 110;
N_z = 110;

%coil area (m^2)

```

```

A_x = 0.0324;
A_y = 0.0324;
A_z = 0.0324;
%maximum current (A)
i_max = 0.49;

%maximum M (Am^2)
M_max = N_x*A_x*i_max

%-----%
% Disturbances %
%-----%

%Solar radiation (worst case scenario) have no effect on LEO satellite

%gravity gradient torque

mu=3.986*10^14;
Ro = 7.221*10^6;
theta = pi/4;

T_grav = ((3*mu)/(2*Ro^3))*(-1*(Inertia(3)-Inertia(1)))*sin(2*theta);

%Aerodynamics torque ignored as well as its a LEO satellite

%Internal torque 10% of generated torque

T_mag = 1*10^-6;

%resultant torques

T_total = 0+T_grav + 0 + T_mag;

Abstract B: Misc

%the magnitude of control torque

mb = T_total/(5*10^-5);

% Programme to generate file of Satellite Position and Earth Mag Field
% wrt earth centred celestial reference frame. (Inertial frame).
% Position in: Rad dist(km) Latc(deg) Lonc(deg)
% Earth's Mag Field in Bxc, Byc, Bzc, (uT)

```

```
% Calls SGP_AO51, B_earth
```

```
clear all
```

```
% Enter the orbit points required
```

```
day = 10; % 10 days after epoch (23 May)
```

```
% Same orbit as in Predict_b2
```

```
dt = 10; % One orbit of AO51
```

```
Pos = SGP_AO51versionb(day,600,dt);
```

```
Fld = zeros(600,3);
```

```
% Calculate fiewos
```

```
%ld over orbit
```

```
for n = 1:600
```

```
    % Find field
```

```
    B = B_earth(Pos(n,1),90-Pos(n,2),180+Pos(n,4));
```

```
    % Convert to XYZ components
```

```
    theta = (pi/180)*(90-Pos(n,2));
```

```
    phi = (pi/180)*Pos(n,3);
```

```
    H = [sin(theta)*cos(phi) cos(theta)*cos(phi) -sin(phi);...
```

```
         sin(theta)*sin(phi) cos(theta)*sin(phi) cos(phi);...
```

```
         cos(theta) -sin(theta) 0];
```

```
    Fld(n,1:3) = (H*B)'; % Convert to XYZ co-ordinates
```

```
end
```

```
Pos_Fld = [Pos(:,1:3),Fld];
```

```
save temp1 Pos_Fld
```

```
function field=B_earth(r,theta,phi)
```

```
% Function to compute Radial, Theta, Phi components of
```

```
% Earth's Magnetic Field (nT) at single point.
```

```
% Note theta = 90-latitude, phi = 180+longitude
```

```
% These theta & phi are for sph polars and phi is different to one used in IGRF10.
```

```
% Note at Auckland,
```

```
latitude = -36.6;
```

```
longitude = 175;
```

```
theta = 90-latitude;
```

```
phi = 180+longitude;
```

```
latrad = pi*(90-theta)/180;
```

```
longrad = pi*(phi)/180; % Note 180deg ADDED
```

```
% World Magnetic Model coefficients
```

```
t = 2.5; % Decimal time in yr from Yr 2005
```

```
wmm_coef = [-295568 0 80 0; -16717 50798 106 -209; -23406 0 -151 0;
```

```
30469 -25947 -78 -232; 16570 -5167 -8 -146; 13354 0 4 0;
```

```

-23051 -1999 -26 50; 12467 2693 -12 -70; 6740 -5242 -65 -6;
9198 0 -25 0; 7981 2815 28 22; 2113 -2260 -70 16; -3794 1458 62 58;
1000 -3047 -38 1; -2274 0 -28 0; 3546 424 7 0; 2087 1798 -32 17;
-1365 -1230 -11 21; -1683 -195 1 48; -141 1036 -8 -11; 732 0 -7 0;
697 -203 4 -6; 767 547 -3 -19; -1512 636 23 -4; -149 -634 -21 -5;
146 -1 -6 -3; -863 504 14 7; 801 0 2 0; -745 -615 -1 6; -14 -224 -3 4;
385 72 11 2; 124 254 6 3; 95 110 5 -8; 57 -264 -4 -2; 18 -51 6 1;
249 0 1 0; 77 112 3 -2; -116 -210 -4 1; -69 96 3 3; -182 -198 -3 4
100 161 2 1; 92 77 4 -2; -116 -129 -7 4; -52 -2 4 4; 56 0 0 0;
99 -201 0 0; 35 129 0 0; -70 126 0 0; 51 -67 0 0; -108 -81 0 0
-13 8 0 0; 88 29 0 0; -67 -79 0 0; -91 60 0 0; -23 0 0 0; -63 24 0 0;
16 2 0 0; -26 44 0 0; 0 48 0 0; 31 -65 0 0; 4 -11 0 0; 21 -34 0 0;
39 -8 0 0; -1 -23 0 0; -23 -79 0 0; 28 0 0 0; -16 3 0 0; -17 12 0 0;
17 -8 0 0; -1 -25 0 0; 1 9 0 0; -7 -6 0 0; 7 -27 0 0; 18 -9 0 0;
0 -13 0 0; 11 -20 0 0; 41 -12 0 0; -24 0 0 0; -4 -4 0 0; 2 3 0 0;
8 24 0 0; -3 -26 0 0; 11 6 0 0; -5 3 0 0; 4 0 0 0; -3 0 0 0; -3 3 0 0;
-1 -9 0 0; -3 -4 0 0; -1 8 0 0];
wmm_coef = 0.1*wmm_coef;

```

```

latinc = pi/360; % Increment used for calculating gradient
a = 6371.2; % Standard Earth Reference radius in km

```

```

% Find X, Y, Z components

```

```

Xt=0;
Yt=0;
Zt=0;
for n=1:12
    SP=legendre(n,sin(latrad),'sch');
    SPgradu=legendre(n,sin(latrad+latinc),'sch');
    SPgradl=legendre(n,sin(latrad-latinc),'sch');
    nn = n*(n+1)/2;
    Xm=0;
    Ym=0;
    Zm=0;

```

```

function Pos = SGP_AO51(day,n,dt)
% Function to give radial dist(km), latc (deg), longc (deg), lon (deg)
% at points along satellite orbit.
% Start time after epoch : day (unit = day)
% Number of points : n
% Time increment between points = dt (unit = sec)
% Uses SGP model
% Calls LoncGrch
n = 600;
day = 3;
dt = 2;

```

% Orbit parameters (KEPs) at epoch

```
to = 6143.69622809; % Time of epoch (23/May/06)
eo = 0.0083636; % Eccentricity of orbit
io = 98.1662; % Inclination of orbit (deg)
Mo = 76.7305; % Mean Anomaly (deg)
no = 14.40518960; % Mean motion (rev/day)
dnodt = 0.00000036; % Rate of change of Mean motion (rev/day/day)
d2nodt2 = 0; % Acceleration of Mean motion (rev/day/day/day)
wo = 282.4533; % ARGP (deg)
Wo = 196.8473; % RAAN (deg)
```

% Find celestial longitude of Greenwich at time of epoch

```
ne = 360.98564736629; % Rotation of earth (deg/day)
lonc_grn = LoncGrch(to);
```

% Constants

```
ae = 6378.135; % Earth radius (km)
a1 = (8681660.4/no)^(2/3); % Approx major semi-axis (km)
cJ2 = 0.5*0.00108263*(ae/a1)^2; % 0.5*J2*(ae/a1)^2
J3rJ2 = -0.00234507; % Ratio of J3 to J2
d1 = 1.5*cJ2*(3*cos(pi*io/180)^2-1)/(1-eo^2)^1.5;
ao = a1*(1-d1/3-d1^2-(134/81)*d1^3); % Major semi-axis at epoch
po = ao*(1-eo^2);
qo = ao*(1-eo);
Lo = Mo + wo + Wo;
dWdt = -3*cJ2*(a1/po)^2*360*no*cos(pi*io/180); % deg per day
dwdt = 1.5*cJ2*(a1/po)^2*360*no*(5*cos(pi*io/180)^2-1); % deg per day
```

```
Pos = zeros(n,4);
```

```
for m = 1:n
```

```
    t = day + (m-1)*dt/86400;
```

% Secular perturbations

```
a = ao*(no/(no+dnodt*t+0.5*d2nodt2*t^2))^(2/3); % Major sem-axis
if a > qo, e = 1-qo/a; else e = 1e-6; end
p = a*(1-e^2);
Wso = Wo + dWdt*t; % RAAN
wso = wo + dwdt*t; % Arg perigee
Ls = Lo + (360*no+dwdt+dWdt)*t + 360*((dnodt/2)*(t^2) + (d2nodt2/6)*(t^3)); % Full anomaly
```

% Convert angles to radians

```
Lsr = (pi/180)*Ls; Wsor = (pi/180)*Wso;
wsor = (pi/180)*wso; ior = (pi/180)*io;
ayNSL = e*sin(wsor) - 0.5*(J3rJ2)*(ae/p)*sin(ior);
axNSL = e*cos(wsor);
Lr = Lsr - 0.25*(J3rJ2)*(ae/p)*axNSL*sin(ior)*((3+5*cos(ior))/(1+cos(ior)));
```

% Solve Keplers equn

Ur = Lr - Wsor; % Eccentric anomaly (initial)

Ewr = Ur;

Ewor = Ewr+1;

while abs(Ewr-Ewor) > 0.0000001

Ewor = Ewr;

dEwor = (Ur-ayNSL*cos(Ewor)+axNSL*sin(Ewor)-Ewor)/(1-ayNSL*sin(Ewor)-axNSL*cos(Ewor));

Ewr = Ewr + dEwor;

end

% Intermediate partially osculating quantities

ecosE = axNSL*cos(Ewr) + ayNSL*sin(Ewr);

esinE = axNSL*sin(Ewr) - ayNSL*cos(Ewr);

eL2 = axNSL^2 + ayNSL^2;

pL = a*(1-eL2);

r = a*(1-ecosE);

sinu = (a/r)*(sin(Ewr)-ayNSL-axNSL*esinE/(1+sqrt(1-eL2)));

cosu = (a/r)*(cos(Ewr)-axNSL+ayNSL*esinE/(1+sqrt(1-eL2)));

ur = atan(sinu/cosu);

if cosu<0 ur = ur + pi; end

% short period perturbations are now included

rk = r + 0.5*cJ2*(a1^2/pL)*sin(ior)^2*cos(2*ur);

ukr = ur - 0.25*cJ2*(a1/pL)^2*(7*(cos(ior))^2-1)*sin(2*ur);

Wkr = Wsor + 1.5*cJ2*(a1/pL)^2*cos(ior)*sin(2*ur);

ikr = ior + 1.5*cJ2*(a1/pL)^2*sin(ior)*cos(ior)*cos(2*ur);

% Calculate unit position vector wrt Celestial XYZ axes

M = [-sin(Wkr)*cos(ikr) cos(Wkr)*cos(ikr) sin(ikr)];

N = [cos(Wkr) sin(Wkr) 0];

U = M*sin(ukr) + N*cos(ukr);

% Calculate position in terms of Radial dist, latC & lonC

rad = rk;

latc = (180/pi)*asin(U(3));

rx = sqrt(U(1)^2 + U(2)^2);

lonc = (180/pi)*acos(U(1)/rx);

if U(2)<0

lonc = -lonc;

end

% Transform Celestial longitude to terrestrial longitude by -

% subtracting celestial longitude of Greenwich and angle of

% earth's rotation since epoch.

lon = lonc - lonc_grn - ne*t;

```
lon = lon - 360*fix(lon/360); % Bring into 360 deg range
if lon <= -180
    lon = lon + 360; % Bring into -180 > +180 range
elseif lon > 180
    lon = lon - 360;
else end

Pos(m,:) = [rad,latc,lonc,lon];
end
```